

AD 697 103

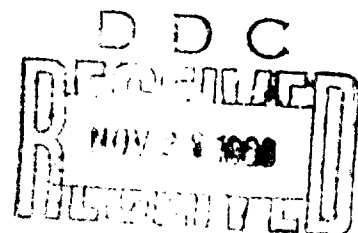
ECOM - 5271
October 1969

AD

GLOBAL ELECTRICAL CURRENTS

By

Willis L. Webb



13

ATMOSPHERIC SCIENCES LABORATORY
WHITE SANDS MISSILE RANGE, NEW MEXICO

U.S. ARMY
CLEARINGHOUSE
FOR THE ARMY
AND AIR FORCE
AND NAVY
AND MARINE CORPS
AND COAST GUARD
AND SPACE FORCE

Distribution of this
report is unlimited

ECOM

UNITED STATES ARMY ELECTRONICS COMMAND

GLOBAL ELECTRICAL CURRENTS

By

Willis L. Webb

ECOM-5271

October 1969

DA Task 1T061102B53A-18

ATMOSPHERIC SCIENCES LABORATORY
WHITE SANDS MISSILE RANGE, NEW MEXICO

Distribution of this
report is unlimited.

GLOBAL ELECTRICAL CURRENTS

ABSTRACT

The atmospheric electrical structure of the earth is postulated to be controlled by a motivating force in the lower ionosphere which is produced by interaction between neutral atmosphere tidal circulations and the ionospheric plasma in the presence of the earth's magnetic field. Associated electric fields power the dynamo currents through the Hall effect with a resulting development of a gross electric potential distribution in the lower ionosphere. Asymmetries in these hemispheric potential distributions result in exospheric current flows in low L-shells, and larger differences in potential produced by dynamo return current flows in high magnetic latitudes result in strong currents through high L-shells between auroral zones. Vertical thunderstorm currents with their associated lightning discharges effectively connect the earth to a low potential region of the dynamo circuit and thus supply the earth with an average negative charge which motivates a leakage tropospheric electrical circuit. In addition, the dynamo currents maintain the magnetic polar regions at different potentials with a resulting electrical exchange with the solar wind through the earth's near space. These considerations indicate that observed electrical and variable magnetic phenomena near the earth are all part of a single comprehensive electrical current system.

CONTENTS

	Page
ABSTRACT - - - - -	111
INTRODUCTION - - - - -	1
GLOBAL CIRCUITRY - - - - -	1
THE DYNAMO DRIVING FORCE - - - - -	3
TROPOSPHERIC ELECTRICAL STRUCTURE - - - - -	5
EXOSPHERIC ELECTRICAL STRUCTURE - - - - -	14
CONCLUSIONS - - - - -	20
REFERENCES - - - - -	21

1. Introduction

A comprehensive concept of the earth's electrical structure has been derived (Webb, 1968b) which provides a framework into which known electrical phenomena may be fitted. A principal item in this new concept is the nature of the motivating force which powers this global electrical system. This power source is hypothesized to result from interaction between the neutral and ionized components of the lower ionosphere, a process which derives its energy from the stratopause thermal tidal circulations. Many details of this concept have not been investigated, in part because of the deep divisions which have developed between various segments of the geo-sciences which are integrated by the concept. It is attempted here to delineate the overall picture in a form which will facilitate comprehensive consideration of the concept.

In addition, further analysis of the basic physical processes which produce the general motivating force is presented. These considerations support the concept of a unified global structure, as opposed to the past theories which have separated the earth's electrical structure into more or less independent telluric (Chapman and Bartels, 1962), tropospheric (Chalmers, 1967), lower ionosphere dynamos (Chapman and Bartels, 1962), auroral and airglow (Chamberlain, 1961) and exospheric currents (Hines, et al., 1965). The several physical processes which have been postulated in attempts to understand these phenomena separately are not questioned at this point. It is presumed, however, that these processes are secondary to the global structure, even though specific processes may exert a firm local control.

2. Global Circuitry

The global electrical circuitry model postulated here is illustrated in Fig. 1. The time selected for this presentation is at noon during the summer solstice of the Northern Hemisphere, when, for geometric and other reasons, conjugate points will generally exhibit higher electric potentials in the Northern Hemispheric dynamo regions. The nomenclature employed in Fig. 1 is:

- R - resistance
- I - current
- t - telluric circuits
- n - Northern Hemisphere
- s - Southern Hemisphere
- f - fair-weather vertical circuits
- c - convective vertical circuits
- h - high latitudes
- ℓ - midlatitudes
- d - zonal dynamo circuits
- e - equatorial
- l - inner radiation belt circuit

- 2 - outer radiation belt circuit
3 - solar wind circuit

The basic driving force is oriented west-east near the 100 km level in low latitudes of each hemisphere during local daytime. This force drives the dynamo currents (I_d) of more than 10^5 amperes which produce a complex electric potential distribution in the lower ionosphere with hemispheric differences of the order of 10^6 volts. The earth, located approximately 100 km under the spherical shell which contains the dynamos, is connected to the dynamo circuits by vertical convective currents (I_c), principally in late afternoon and evening at low latitudes where the dynamo potentials are negative relative to noontime. This geometry impresses an observed negative charge of more

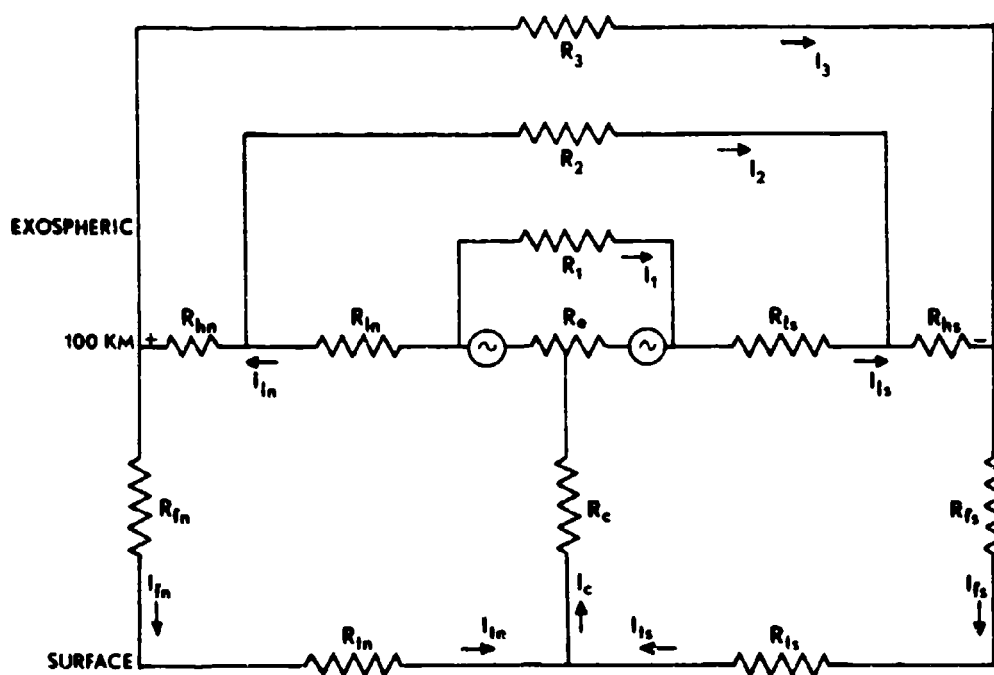


Figure 1. Schematic Diagram of the Global Electrical Circuitry for the Local Noon Meridian.

than 10^5 coulombs on the earth, which in turn produces an approximately symmetrical 10^3 amperes vertical current (I_v) through the fair-weather semiconducting lower atmosphere with associated telluric currents (I_t) through the earth's crust to thunderstorm regions.

In general, the electric potentials at conjugate points of the two hemispheres will not be equal. In low latitudes exospheric currents (I_1) will flow along magnetic field lines principally to relax potential differences imposed by differences in the basic dynamo driving forces. Auroral zone hemispheric potential differences will produce larger exospheric currents (I_2) at high magnetic latitudes, principally as a result of the asymmetry between the rotational and magnetic systems.

The final supplementary current path is formed by interaction of the earth's magnetosphere with the solar wind. Polar regions of the lower ionosphere will be maintained at different electrical potentials by the dynamo currents, and currents (I_3) through the solar wind plasma will result. It is probable that the geo-segment of this circuit will incorporate the I_2 circuit. During strong solar disturbances this current is known to become intense, approaching the 10^5 amperes of the dynamo circuits, although in general the exospheric currents are orders of magnitude smaller than the dynamo currents.

The earth's global electrical structure is then established by the potential field of the dynamo currents. Tropospheric and exospheric electrical structure is formed by leakage current paths which are controlled by the basic dynamo potentials.

3. The Dynamo Driving Force

The dynamo currents represent the principal geo-electric phenomenon, with average intensities which are two orders of magnitude greater than other circuits. An understanding of the earth's electrical structure requires that the force which drives these lower ionosphere currents be clearly delineated.

A new attempt at this problem has been made by Webb (1968a, 1968b, 1969) based on an assumed net vertical motion imposed on the upper atmosphere by tidal circulations of the stratopause regions. The characteristic cold mesopause indicates, in agreement with other observations, the presence of turbulent flow in the mesosphere to transport heat downward through adiabatic processes. A model of the general daytime vertical structure of molecular and eddy transport coefficients based on limited amounts of data (Lettau, 1951; Booker, 1956; Zimmerman and Champion, 1963; Kellogg, 1964; Johnson and Wilkins, 1965) is presented in Fig. 2. Higher values of eddy transport coefficients have been reported in the 80 to 150 km region (Zimmerman and Champion, 1963) but the molecular diffusion stratification which is observed above approximately 105 km (Blamont and de Jager, 1961) indicates that a portion of the observed values may result from electrically forced diffusion of the ionized trail sensors. These considerations then indicate

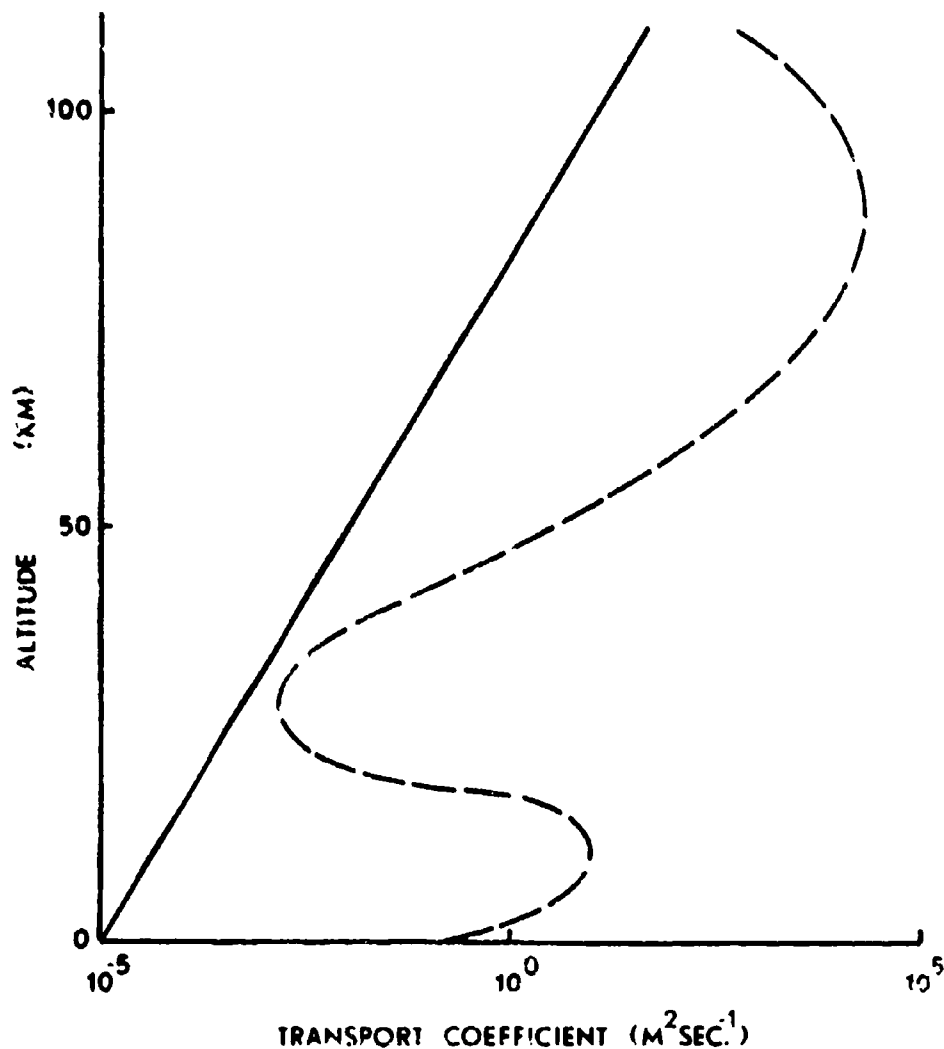


Figure 2. Model Molecular (solid curve) and Eddy (dashed curve) Diffusion Profiles

that the 70-100 km region is characterized by eddy transport coefficients in the range of $10^3 - 10^5 \text{ m}^2\text{sec}^{-1}$.

Now the daytime electron-positive ion concentration (n) in the 70-100 km region varies over roughly three orders of magnitude, with a 100 km value of approximately 10^{11} electrons and positive ions per cubic meter. Negative charged particle lapse rates of $5 \times 10^6 \text{ p m}^{-4}$ at 100 km, $8 \times 10^5 \text{ p m}^{-4}$ at 90 km and 10^5 p m^{-4} at 80 km with this eddy transport (Fig. 2) will produce a downward flux of collision-controlled charged particles given by the relation

$$F = - D_e \frac{\partial n}{\partial h} . \quad (1)$$

As has been pointed out before (Fejer, 1965; Webb, 1968b), in this region of the atmosphere collision processes will transport positive ions but are ineffective in transporting electrons. Downward transport of positive ions by these eddies in an electrically neutral atmosphere will effect charge separation at a nominal velocity given by

$$v = \frac{F}{n} \quad (2)$$

The nominal downward velocities of positive ions under the above conditions will then be of the order of 1 mps at 80 km, .8 mps at 90 km and .5 mps at 100 km.

As was shown by Webb (1968b) such charge separation will, in equatorial regions, result in production of an upward-directed electric field which will force positive ions to migrate upstream with an equal speed so that electrical equilibrium is achieved. This latter situation is described by the relation

$$qE = M\omega v \quad (3)$$

where q is the particle charge, E is the equilibrating electric field, M is the particle mass, v is the collision frequency and w is the particle velocity relative to the medium. The data presented above with the assumptions of Webb (1968b) indicate that electric fields directed upward with maximum intensity of 0.2 v m^{-1} at 80 km will be generated by this mechanism. At night this mechanism will be reduced in intensity by approximately two orders of magnitude as a result of a similar decrease in electron density. This situation has been shown (Webb, 1968a; 1968b) to be adequate to produce, through the Hall effect, an electric potential field which is consistent with known electrical phenomena of the region.

The above discussion and that of Webb (1968b) indicate that the driving forces of the dynamo currents are reasonably derived from vertical charge separation produced by collision processes in the circulations and turbulence produced by the stratopause thermal tides.

4. Tropospheric Electrical Structure

The fair-weather electrical structure of the lower atmosphere has been extensively explored (Chalmers, 1967). It is variable, with a general resistivity vertical structure of the type illustrated in Fig. 3 (Cole and Pierce, 1965). Here the bulk resistivity of the air exhibits its characteristic high value near the surface, decreasing rapidly with height so that the vertical path resistance is established by the resistance of the lower few kilometers. Almost 98% of the total vertical path resistance of roughly $1.8 \times 10^{17} \text{ ohm m}^2$ is obtained in the first 10 km, and almost 90% is obtained in the first 5 km.

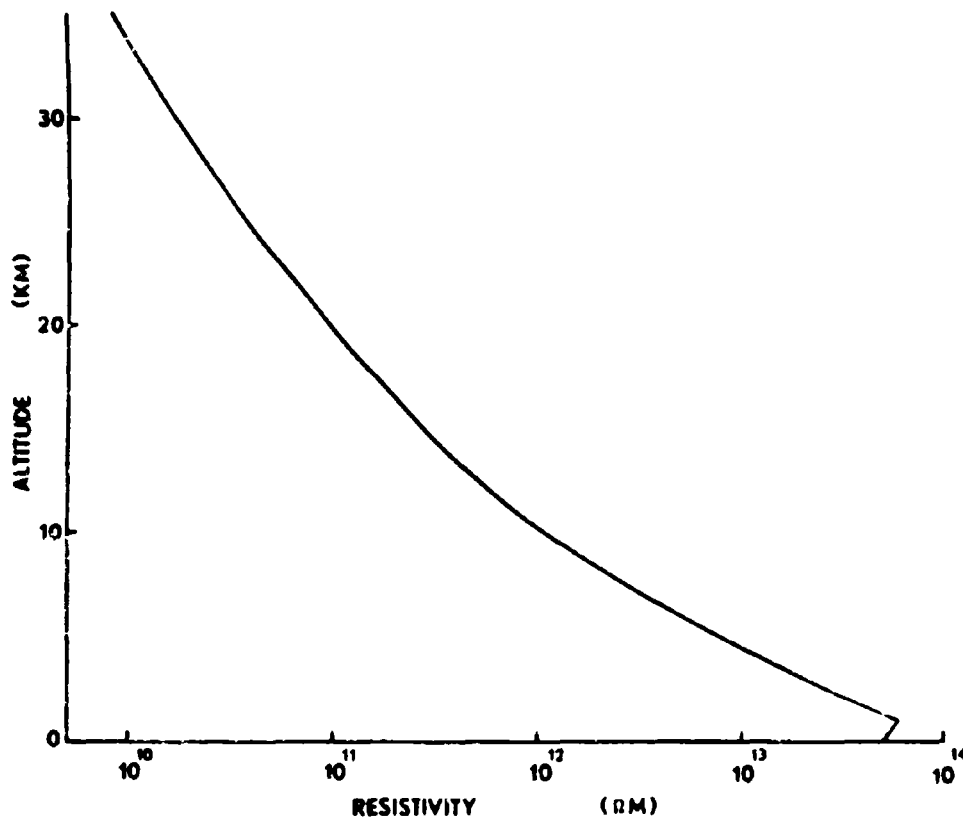


Figure 3. Typical Low-Latitude Vertical Resistivity Structure of the Troposphere and Lower Stratosphere.

In the stable fair-weather case, the vertical distribution of atmospheric space charge which produces the observed change in potential gradient can be calculated approximately from the relation

$$\rho = -\epsilon_0 \frac{\partial^2 V}{\partial h^2}, \quad (4)$$

where V is the electric potential, and $\epsilon_0 = 8.854 \times 10^{-12}$ farads per meter is the permittivity of free space. Neglecting horizontal currents, the fair-weather electric current of the lower atmosphere will be constant with height, and, to a good approximation (Ohm's law), the potential distribution has the character of the resistivity curve of Fig. 3, with an overall potential difference of approximately 3×10^5 volts. By applying Eq. 4 to these data, a representative vertical fair-weather space charge distribution is obtained as illustrated in Fig. 4. Clearly, the positive space charge of the atmosphere which must face the observed surface charge density of approximately -8.8×10^{-10} coulombs m^{-2} is principally contained in the lower troposphere. The traditional leaky capacitor concept of fair-weather electrical structure is thus modified to include a diffuse upper

plate located in the lower troposphere. The fair-weather troposphere capacitor plate contains a total positive space charge of approximately 400,000 coulombs, with a roughly equal negative charge on the surface of the earth. In addition, the vertically integrated space charge of the dynamo region (75 - 120 km) of roughly 10^{-14} coulombs m^{-2} is negligible compared to these tropospheric space charges.

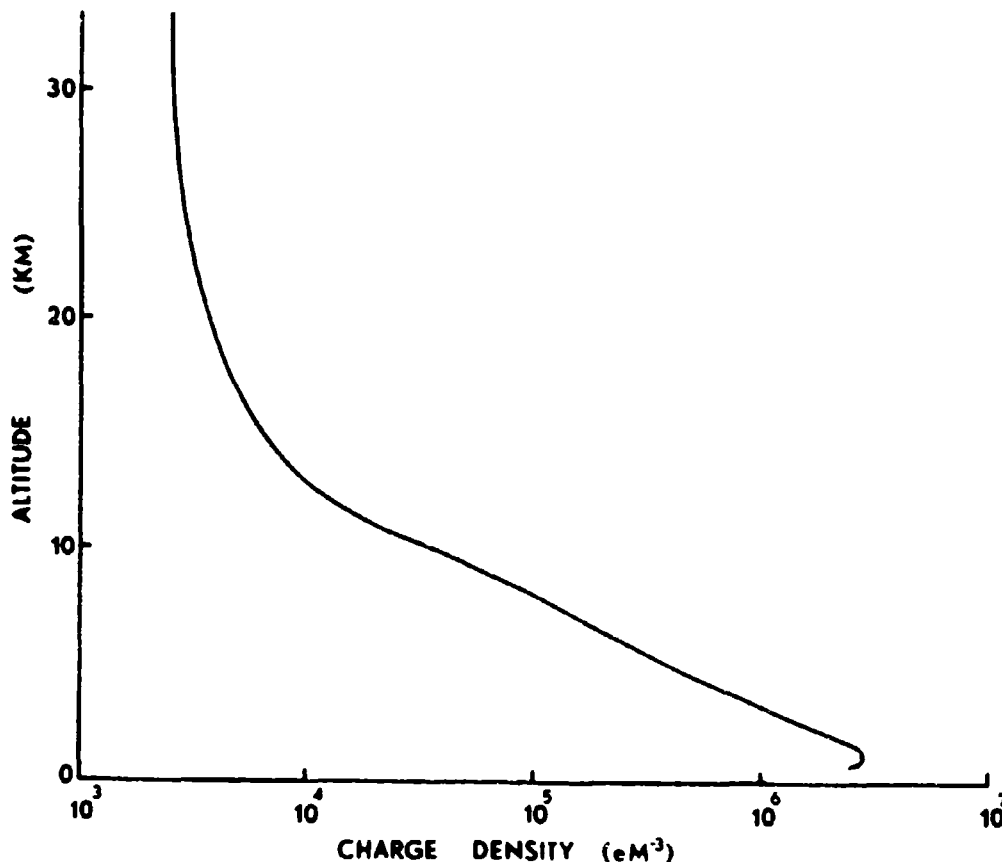


Figure 4. Typical Low-Latitude Vertical Structure of the Atmospheric Fair-Weather Positive Electric Space Charge.

The very low electrical mobility of most tropospheric ions in the boundary layer indicates that, in the presence of the general fair-weather potential gradient, electrically forced molecular diffusion will be, on occasion, exceeded in intensity by eddy diffusion. Mixing produced by thermal and frictional effects may dominate electrical physical processes under certain conditions so that the electrical structure which results frequently deviates from the simple picture of a homogeneous, stratified, static fair-weather field which is assumed above.

Certain features of the tropospheric electrical structure are comparatively static. This is true of any high impedance circuit, however, and does not alter the basically dynamic nature of earth electrification. The gross capacitance and charge of the earth's tropospheric electrical system ($C \sim 1$ farad) and small vertical current densities (approximately 2×10^{-12} amperes m^{-2}) of the troposphere effectively filter the variable aspects of atmospheric electricity, shielding the surface layers from the very dynamic aspects of higher levels.

The fair-weather capacitor electrical structure described above is effectively disrupted by occurrence of convective systems. Air that is rich in positive charge (Fig. 4) is assembled by the lateral flow, immobilized by droplets at low levels (1-2 km), and transported vertically by these convective systems in a thin column which spans the lower 10-25 km of the atmosphere as is illustrated in Fig. 5. The relatively low

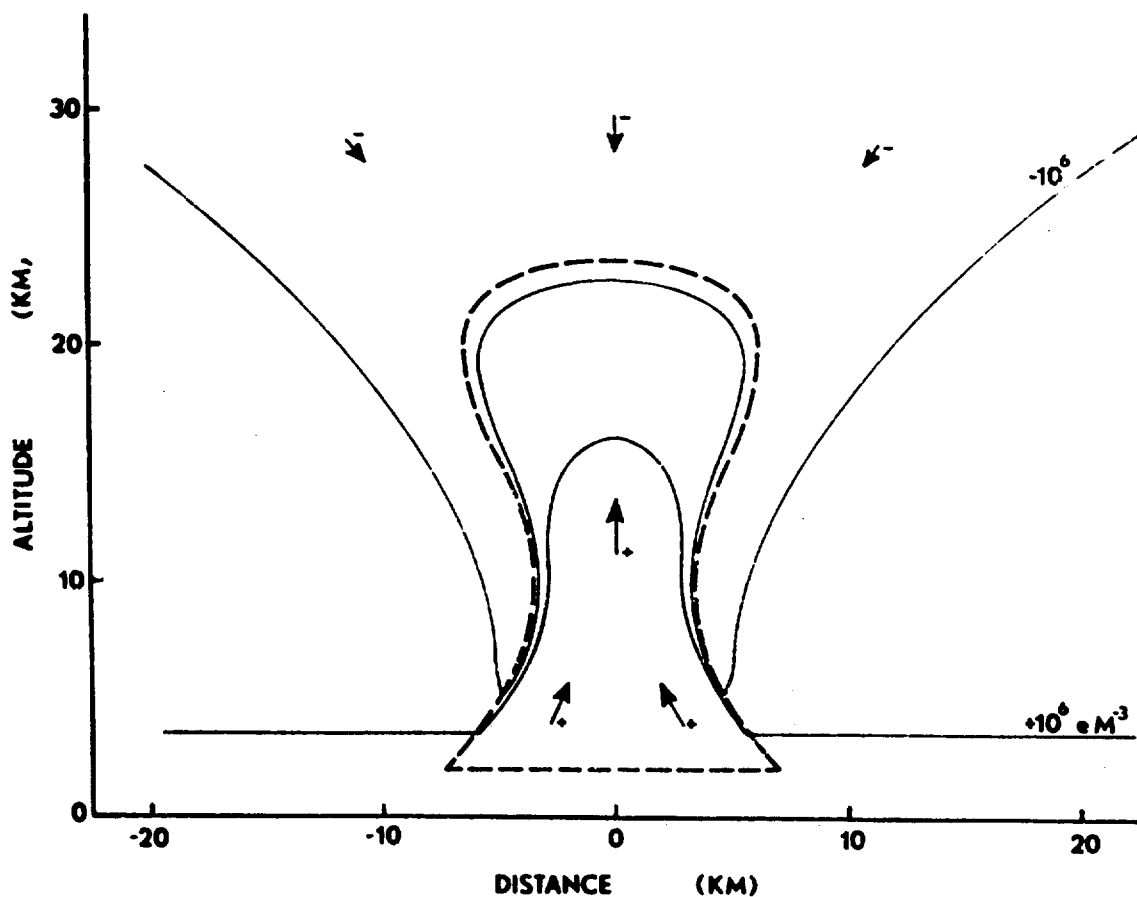


Figure 5. Initial space charge distribution associated with a convective cell before the dynamo potentials become involved. The dashed curve indicates the structure of the cloud, and the arrows indicate net motions of charged particles.

mobilities of tropospheric electrical charges are generally reduced drastically by condensation processes so that characteristic surface boundary layer electrical time constants of tens of minutes are effectively extended to beyond the half-hour lifetime of the average convective storm. If a 14 mps mean vertical flow through a 7 km diameter throat of a convective cloud (Goldman, 1968) with 10^6 excess positive charges per cubic meter (Fig. 4) is assumed, the more intense convective systems will transport approximately 10^{-4} coulombs of resident positive charge upward each second. A first response to this positive convective current will be an intensification of the fair-weather type field under the cell as the positive space charge converges. Rapidly, however, neutralization of this convection-borne positive space charge relative to the earth will be accomplished by negative ions in the upper atmosphere so that the negative surface charge on the ground under the cell will stabilize.

Introduction of this charge structure into the upper troposphere and lower stratosphere will result in strong response by the highly conducting upper atmosphere. Relaxation time constants ($T = \frac{\epsilon_0}{\sigma}$, σ - conductivity, Chalmers, 1967, p. 39) of approximately 100 seconds at 5 km, 20 seconds at 10 km, 4 seconds at 15 km and one second at 30 km in clear air around the thunderstorm may be expected. Upward transport of a cylindrical column of air containing roughly one coulomb of positive charge into the 5-15 km region of the storm can be expected to very quickly result in flow of an equal negative charge onto the edge of the cloud in the lower atmosphere. The mobility of the charge carriers in this conduction current will also decrease drastically when they enter the cloud as a result of capture by cloud droplets. This process will result in development of a thin sheath of negative charge around the positive core of the storm. The intruding positive space charge may then be eliminated by discharges within the cloud between these centers of charge concentration or by recombination at the top of the cloud where the cloud particles evaporate.

The capacitance of this vertical cloud system per unit length can be estimated by the relation for specific capacitance of a cylindrical capacitor with inner plate at radius a and outer plate at radius b (Wilson, 1958)

$$c = \frac{2\pi \epsilon_0 \epsilon}{\ln(\frac{b}{a})} \quad (\text{farads per meter}) \quad (5)$$

Using values of $\epsilon = 1$, $a = 3.25$ km and $b = 3.5$ km, the capacitance of this vertical cloud system is found to be approximately 7×10^{-10} farads m^{-1} . This estimate indicates that the positive space charge of the fair-weather field near the surface will supply a specific positive charge concentration (q) of approximately 2×10^{-6} coulombs per meter length of the cloud. The equilibrium electric potential of the inner cylinder which results from this

central charge can be approximated by (Wilson, 1958)

$$V_a = \frac{q}{2\pi \epsilon_0 \epsilon} \ln \left(\frac{b}{a} \right) \quad (\text{volts}) \quad (6)$$

which yields approximately 3×10^3 volts.

The boundary of the storm cloud will acquire a neutralizing negative charge resulting from a downflow of negatively charged particles from the highly conducting dynamo region above the storm. This electric current, which is directed upward, must have a magnitude of 10^{-4} amperes to match the upwelling positive current in the cloud. This vertical current has important implications for the electrical structure of the lower atmosphere and the earth's surface. Our electrostatic structural assumptions of the fair-weather situation are immediately invalidated as this upward current punctures the earth-troposphere capacitor, and the following two major conditions will prevail:

a. There will be a $V = IR$ voltage drop along the current path from the storm cloud to the dynamo circuit above. Nominal values of $I = 10^{-10}$ amperes m^{-2} and $R = 10^{15}$ ohm m^2 give potential drops of 10^5 volts, with the top of the storm at the higher potential.

b. The top and sides of the cloud will assume the potential of the dynamo current above the storm plus the difference of (a). This latter item is of major importance, since it has been shown (Webb, 1968b) that the potential drops of the dynamo currents introduce gross horizontal potential variations of the order of 10^6 volts into the global electrical structure of the lower ionosphere. Thus, the storm cloud upwelling of positive charge from the fair-weather field discussed above will have the net result of adjusting the potential of the outer margins of a convective cloud down to altitudes of 1-2 km toward the gross potential of the dynamo region above the storm.

Stergis, Rein and Kangas (1957) have measured the potential gradient and conductivity near 20 km above thunderstorms from the direct current point of view, obtaining results indicating an upward current of the order of one ampere over each storm with maximum negative potential gradients of a few hundreds of volts per meter. Using 200 volts m^{-1} at 20 km, 50 volts m^{-1} at 25 km and the resistivity curve of Fig. 3, the potential drop in this current path approximates 5×10^5 volts under steady-state conditions.

When the dynamo potential above a convective cloud is negative relative to noontime (late afternoon and nighttime; Webb, 1968b), a positive surface charge will be impressed on the earth's surface in the vicinity of the convective cloud, the tropospheric electric field will reverse sign relative to the general fair-weather situation and the potential

difference between the earth's surface and the outer margins of the cloud will be double that of the dynamo circuit to which the storm is connected. Introduction of negative dynamo potentials of the order of 6×10^5 volts or greater to near the earth's surface will induce coronal discharge of positive charge (Chalmers, 1967, Chapter 9). With development of convective systems, enhancements of such space charge by more than three orders of magnitude above the fair-weather values have been observed (Vonnegut, Moore and Botka, 1959). Thus, the 10^{-4} amperes vertical current mentioned above as produced by the fair-weather space charge will be increased to more than 10^{-1} amperes, and the captive charge of the cloud condenser will be increased to more than 10^{-3} coulombs per meter for a total cloud charge of the order of 10-100 coulombs. These values imply general potentials across the cloud condenser system of 10^6 to 10^7 volts, and it is likely that inhomogeneities in the entire process can easily produce the local potentials of 10^8 volts and greater which appear to be required to initiate observed lightning discharges.

The tropospheric return current through thunderstorms must then consist of three modes. The first is upward transport of positive charge in the convective current, and the transport of these charges may represent an added source of energy for the tropospheric electrical circuit. The second is a conduction flow upward outside the convective system involving positive coronal charges migrating upward from the surface and combining with downward-moving negative charges, moving in the forced diffusion mode at higher altitudes and in convective downward motions around the cloud system at low altitudes. The third mode is high intensity upward current flow across the lower atmosphere in intermittent low resistance lightning discharge paths. Convective cells thus establish local electrical structures in which the approaching negative charges from above polarize the earth's surface, producing a negative potential gradient and an upward current flow.

The concept of thunderstorm electrification presented above is parallel to the concepts developed by Grenet, Vonnegut and Moore (Grenet, 1947, 1959; Vonnegut, 1955; Vonnegut et al., 1959; Moore et al., 1962; Vonnegut et al., 1961; Moore et al., 1960; Vonnegut and Moore, 1960; Moore et al., 1958), with the major exception of addition of the horizontally stratified 100 km region dynamo circuit potential to induce corona and activate the electrical processes of convective cloud systems. Convective energy is necessary in initiating this series of events, but the impact of the dynamo electric potentials is overwhelming. These considerations indicate that the partial agreements which have been obtained by numerous thunderstorm electrification theories (Chalmers, 1967) are simply fortuitous, with the basic tropospheric charge-separating mechanism centering on vertical eddy transport of captive space charge.

The tropospheric electrical circuit elements discussed above require that a portion of the circuit lie in the earth. The diffuse global fair-weather current must converge to a few local storm areas for the return trip through lightning discharges. Elementary physical considerations

indicate that these telluric currents will flow in the surface layers of the earth. Since thunderstorms and their associated lightning events exhibit maximum occurrence at low latitudes in the afternoon and evening, these telluric currents must be generally directed equatorward during the daytime and poleward at night.

Electric currents have been known to exist in the earth's surface since the mid-19th Century. Use of long copper telegraph lines over land regions (a $10^7 - 10^9$ ohm meter reduction in resistivity) indicated the presence of low-latitude potential differences as high as 10^{-5} v m^{-1} over the surface of the earth with their associated currents. Chapman and Bartels (1962) have summarized the early studies of this phenomenon. They indicate resistivities of a few tenths of an ohm meter in sea water and 1-50 ohm meters in moist loam, with an average value of 100 ohm meters for the general topsoil. Increased resistivity with depth in the ocean results from the colder waters of ocean depths. All considerations indicate that telluric currents are a shallow surface phenomenon.

If a 1 km layer is considered representative, the $10^{-7} - 10^{-8}$ amperes m^{-2} which Chapman and Bartels reported for continental areas yield integrated half-day hemispheric telluric currents in the $10^2 - 10^3$ amperes range. This value is low since high-conductivity ocean paths will provide partial shorts for the continental currents. The intensity of telluric currents may thus be considered adequate to supply the consolidated flow from the global fair-weather charge accumulation to the bases of lightning paths. Redding (1967) has pictorially described the diurnal structure of low-latitude telluric currents, showing that they do indeed flow toward low latitudes during the day and toward the poles at night, indicating that they flow toward the region of principal thunderstorm activity.

Severe complications in telluric current observations caused by technique difficulties, local impedance variations and surface charges prevent detailed association of this current segment with the vertical components of the tropospheric electric circuit. Much more information is also required relative to the location of lightning return paths before an adequate understanding can be obtained. It is concluded, however, that telluric currents are indeed adequate to provide the earth circuit segment for the tropospheric current path of the dynamo circuits.

A detailed schematic diagram of the tropospheric electrical circuitry in a vertical low-latitude zonal plane from the high dynamo potential point at 2 P.M. into the low potential region of nighttime is presented in Fig. 6. The principal driving force (with potential differences of the order of 10^6 v) is located at the base of the horizontally stratified dynamo circuit near 80 km altitude (Webb, 1968b). This force causes current to flow from low to high potential and results in accumulation of a diffuse positive space charge in the region marked A ($q \sim 10$ em $^{-3}$). The principal leakage return path for this potential difference is the dynamo current (approximately 10^5 amperes) circuit through high latitudes at the 100 km level, but a secondary tropospheric return current (I , approximately 1500 amperes) circuit is established in the tropospheric mode illustrated in Fig. 6.

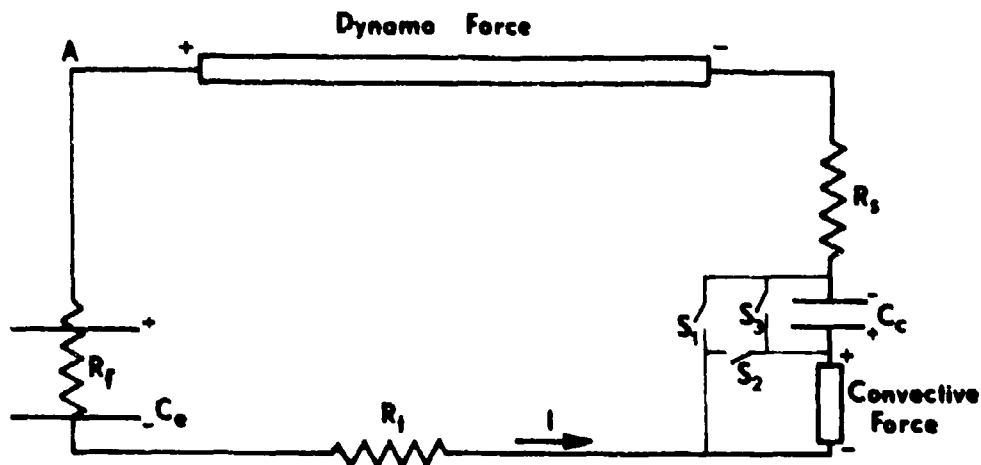


Figure 6. Schematic Circuit of Tropospheric Electrification in a Vertical Low-Latitude Longitudinal Plane from 2 P.M. to after Sunset.

The fair-weather vertical portion of the tropospheric circuit is represented by the resistance R_f and the capacitance C_e . Nominal values of electrical circuit elements in this region are path resistances of 10^{17} ohm m^2 , specific capacitance of 10^{-15} farads m^{-2} , current densities of 2×10^{-12} amperes m^{-2} and 3×10^5 volts overall potential difference (lower at the ground) as was discussed above. Telluric impedances (R_t) yield potential drops of 10^{-6} volts m^{-1} with continental current densities of 10^{-7} amperes m^{-2} in the general case. Stratospheric impedance (R_s) above convective storms appears to be equivalent to that of the stratosphere in other locations (Fig. 3), but the area above a convective storm is the site of larger current densities and thus of larger electric fields.

While the conductivity in a cloud is subject to debate, it will be assumed here that in strong convection, high cloud droplet concentrations ($> 10^9 m^{-3}$) will prohibit effective molecular diffusion of charges so that resistance to electrical current flow in the cloud will become very great, with general cloud characteristics of a condenser (C_c , Fig. 6) of $10^{-5}f$ capacitance for a 20 km length cloud. During initial stages of convective development, the electrical force provided by convective eddy motions will be limited to supplying current flows of the order of 10^{-4} amperes in individual systems. When the convective cloud system becomes effectively connected to the dynamo electrical potential above it, however, coronal discharges from the earth's surface into the low-level air which serves as the source for convective mass transport will strongly enhance the electrical transport process. In this case, the convective transport current will become very strong, possibly contributing significantly to the total current flow of the tropospheric electrical system.

On occasion lightning discharges (S_2 in Fig. 6) may serve to negate this contribution.

Observations indicate that lightning discharges may act as switches (S_1 and S_3 in Fig. 6) to short the charges which accumulate in the cloud-generated open circuit. During the period in which a lightning path exists, the path resistance of the convective segment of the tropospheric portion is reduced many orders of magnitude, and the upward tropospheric current flow will then be through the resistance R_s . When lightning paths exist, the tropospheric leakage current path of the dynamo circuit is

$$R = R_f + R_c + R_s$$

which reduces to $R_c + R_s$ to a good approximation. These are known to be approximately 10^{18} and 10^{16} ohm m², respectively (Fig. 3).

Current densities through these two portions of the tropospheric circuit will be different, however, due to the significant difference in cross-sectional areas of these circuit elements. Peak current densities over severe storms appear to be of the order of 10^2 times the fair-weather values, but reasonable mean values over storm areas would be of the order of ten times greater. This would indicate that the potential drop of the fair-weather leg (R_f) is several times that of the stratospheric branch (R_s). Flow through this voltage divider thus maintains the earth near the average negative potential of the portion of the dynamo circuit under which the convective storms operate.

Since the fair-weather current flow is generally toward the earth even relatively close to thunderstorms, it is clear that the intermittent nature of lightning is of considerable importance. Through this mechanism, the earth is closely related to the mean electrical potential field of the dynamo region above active storms, but the brevity of the events (milliseconds) does not allow the sluggish troposphere (tens of minutes) to approach equilibrium with the new circuit parameters during this special event. The average potential of the earth is thus maintained at a negative value relative to the tropospheric condenser plate by the local dynamic characteristics of this tropospheric circuit.

5. Exospheric Electrical Structure

The vertical distribution of the dynamo currents at low latitudes has been derived by Webb (1968b) from stratospheric tidal circulation data. Chapman and Bartels (1962) and recently Matsushita and Maeda (1965) and Matsushita (1965) have used data on variations in the geomagnetic field to derive the lateral distribution of electric current systems which flow in the upper atmosphere. Under the assumption that these "dynamo" currents are confined to the 100 km region globally by the unique "Pall" and "Pedersen" conductivity profiles it is possible to derive the global current density of that level. Conductivity structures of the 100 km surface may be approximated from published mean electron density data

(Wright, 1962) and magnetic field aspect data (Vestine, et al., 1947) for particular values of collision frequency. Through use of these sources of information it is possible to calculate the electric potential field of the 100 km surface.

The result of such model calculations for Northern Hemisphere fall equinox time is illustrated by the model potential distribution presented in Fig. 7. A high-potential region of the order of 10^6 volts is indicated

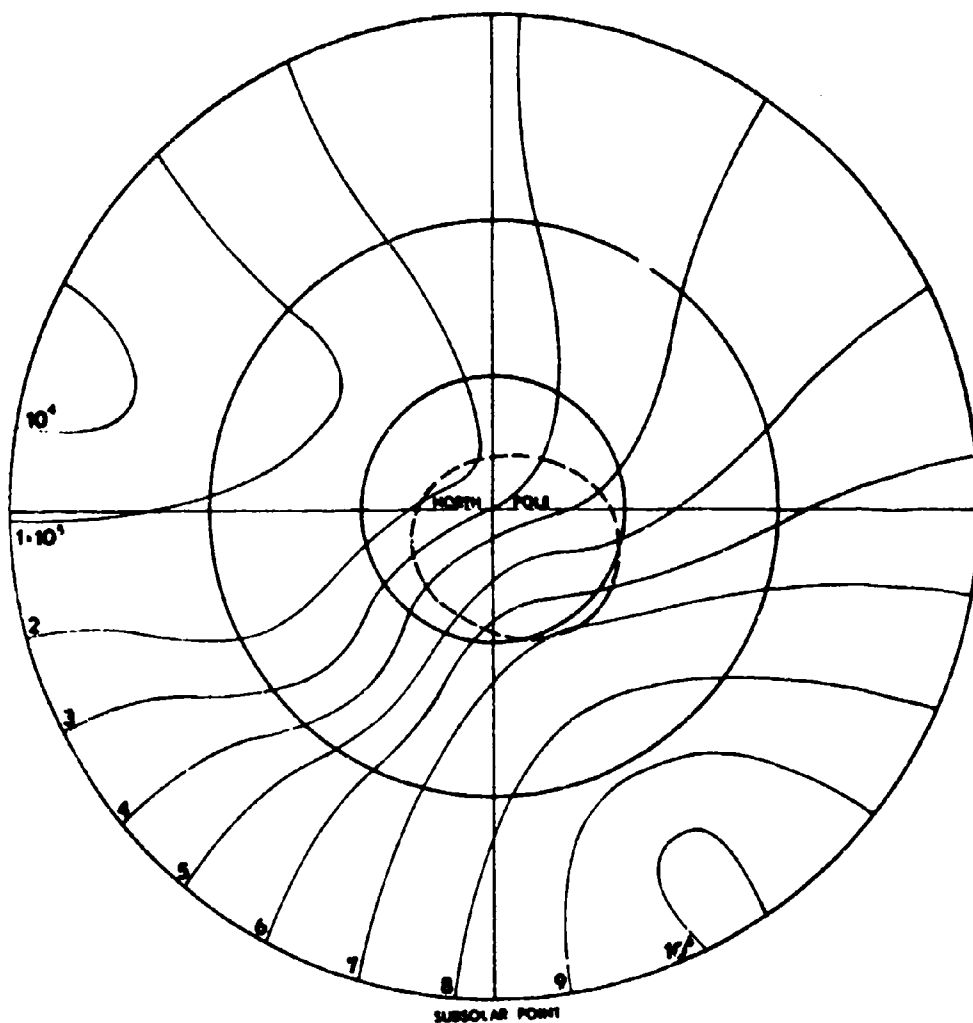


Figure 7. Model electrical potential field for the lower ionosphere at equinox time. Units are volts. The dashed curve represents the auroral oval.

by these considerations to be located in early afternoon low latitudes, with an expansive region of low potential covering nighttime regions. High-latitude auroral regions are indicated to be at intermediate potentials, with considerable variations in potential around the auroral oval. The position of the southern magnetic pole and its auroral oval at the time of Fig. 7 indicates that there will be significant differences in potential of the dynamo regions between conjugate points, even in this relatively symmetric equinox situation.

Consideration of the variations which will be introduced into these hemispheric potential distributions diurnally as a result of rotational and magnetic axes asymmetries indicates that local potentials and conjugate potential differences will vary markedly in the course of a day. In addition, the known gross inhomogeneity of the ionosphere in small scales and the detail structure of the stratospheric tidal circulation and tropospheric lightning perturbations will assure inhomogeneous dynamo currents and thus highly inhomogeneous potential fields. Marked differences will occur at similar geomagnetic latitudes between summer and winter hemispheres as a result of differences in conductivity structure and intensity of the tidal circulations. These differences are in addition to the above-mentioned local and hemispheric variations, with the result that the global potential field of the 100 km level will be very complex indeed. The smoothed curves of Fig. 7 must be interpreted as averaged conditions with gross variations superimposed locally.

All of the above calculations have been based on the assumption that the dynamo circuits are independent current systems which are isolated from other sources or sinks of electrical energy. This is an approximation which, on the lower tropospheric side, has been evaluated (Webb, 1968b) to involve neglect of currents of the order of one percent of the dynamo current system, and thus generally negligible relative to the 100 km dynamo current, and potential structure. An exception is to be noted in the case of short period changes resulting from events such as lightning discharges, where large charge transports (30 coulombs moved 10 km vertically) do introduce gross potential changes for short periods.

Boundary conditions on the upper side of the dynamo currents are less likely to be negligible, however, as a result of currents which may flow in the high conductivity plasma in which are embedded magnetic field lines of the magnetosphere. At some level in the upper ionosphere the known reduction of plasma density and the increase in dynamic impedance (Swift, 1965) with height will reduce the conductivity (increase the resistivity) to the point that substantial electric fields will exist along the magnetic field. These magnetic-field-aligned electric fields will result in acceleration of charged particles to higher energies than are representative of ambient neutral particles and will accelerate the positive and negative particles differently according to mass. In the upper portions of this accelerating region, some of the more favored particles will gain escape velocities and will move out along the magnetic field toward the conjugate point of the other hemisphere where they will execute a reversed but similar program of energy exchange with that upper ionosphere region.

The above described vertical motions will represent new sources and sinks of electric current for the dynamo currents which we have described above and thus modify the potential field of the dynamo region. Under quiescent conditions, these exospheric currents are indicated to be of the order of 10^{-12} am $^{-2}$ (O'Brien, 1964) and thus are reasonably negligible, but there is observational evidence that on occasions of solar disturbances these interhemispheric currents exhibit extreme values of 10^{-5} am $^{-2}$ (Sharp, et al., 1967), and thus may be competitive locally with the dynamo currents in intensity and may introduce gross modifications to the simple E-region potential distribution picture presented in Fig. 7. This is especially to be expected in high latitudes where interaction between the earth and the solar wind can be expected to support large vertical currents.

The dynamo currents of the E-region will be modified by currents flowing through the exosphere in paths formed by the earth's magnetic field and the exospheric plasma. The conductivities of these paths are complex, with charged particle diffusion modes the rule in low altitudes and particle transient modes dominate in the magnetosphere. Buneman (1959) indicates that the magnetospheric longitudinal (along the field) conductivity is given by

$$\sigma_0 = 5.556 \times 10^{-8} \omega_{pe} \quad (7)$$

where ω_{pe} is the plasma frequency of the electrons. This indicates a conductivity of approximately .5 mho m $^{-1}$ in the 500-600 region, decreasing to approximately 10^{-2} at high altitudes.

These values indicate that exospheric path resistances on low L shells (L1) are of the order of 10^9 ohm m 2 , on auroral L shells (L5) of the order of 10^{10} ohm m 2 and in the polar regions of the order of 10^{11} ohm m 2 . These path resistances may be compared with estimated 10^{10} ohm m 2 (Webb, 1968b) resistance of the dynamo 100 km level return current circuit through the auroral zones and the 10^{17} ohm m 2 (Webb, 1968b) resistance of the tropospheric circuit.

In low latitudes, magnetospheric currents will flow as a result of differences in the conjugate potentials of the powered (zonal) and relaxation (meridional) segments of the dynamo circuits. These currents (I_1 , Fig. 8) are in the region of the inner Van Allen belt and are thus assumed to be associated with development of that trapped radiation. These currents act to smooth differences between the hemispheric dynamo current generators.

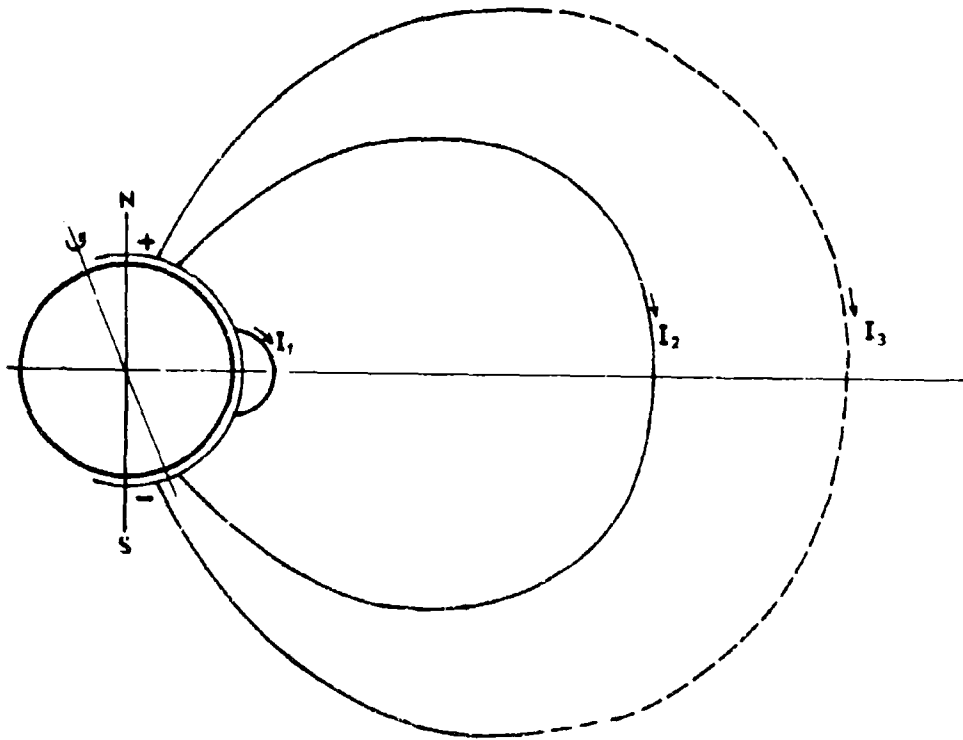


Figure 8. Schematic of exospheric current systems for the case in which the dynamo current potential fields hold the northern magnetic high latitude at a positive potential relative to the Southern Hemisphere.

Zonal flow of the dynamo currents in auroral zone E-regions will result in strong zonal potential gradients around the auroral oval. Inspection of the geometry of the high latitude case (Webb, 1968b) indicates that when the hemispheric dynamo potentials in the driving regions are equal, differing hemispheric meridional path lengths of the dynamo return currents would tend to produce occasional conjugate potential differences of more than 10% of the total dynamo potential gradients, or of the order of 10^5 volts in high latitudes. Exospheric currents along the magnetic field will develop in response to these gradients and tend to reduce them. The result will be current flows (I_2) as is illustrated in Fig. 8.

At high geomagnetic latitudes, the magnetic field lines between hemispheres become electrically completed as a result of interaction with the plasma and magnetic field of the solar wind. Nonlinear acceleration processes will result in potential differences along magnetic field lines, and the interhemispheric potential differences will be reduced with increasing latitudes in polar regions as a result of these current flows. The current

flow in this third magnetospheric current region is designated I_3 in Fig. 8, the dashed portion indicating the uncertain current path through the magnetospheric tail and the solar wind.

These three current systems are assumed to provide support for the ring current which has been hypothesized to circle the earth (Chapman and Bartels, 1962), produced by transverse drift motions imparted to charged particles participating in these magnetospheric currents as a result of accelerating electric fields. The gross geometry of I_3 indicates that it will be ineffective in producing the magnetic effects of the ring current which are observed at the earth's surface. Satellite observations indicate that I_1 is relatively stable. It is concluded, then, that the principal contributor to surface-observed ring current magnetic field changes is probably I_2 , presumably as a result of solar wind currents from I_3 through the high-latitude ionosphere and through the I_2 circuit. The currents through I_3 and I_2 are thus directly modulated by the intensity of the solar wind. This is the "indented current ring" of Akasofu and Chapman (1964). Thus, auroral activity, the ring current and its associated magnetic effects, polar storms and other physical processes associated with I_2 and I_3 will vary with these two controlling processes.

Small-scale variations in the dynamo currents will induce inhomogeneities in the interhemispheric current flows, resulting in strong gradients in these currents with magnetic latitude and longitude. These inhomogeneities in ionospheric potentials will introduce variations in exospheric current densities which can be expected to result in electric fields transverse to the geomagnetic field which will, in turn, result in particle motions normal to the plane of these two vectors. Transport of plasma into and/or out of the plasmasphere may be expected to result.

Measurements of precipitation currents in the ionosphere indicate general values of approximately 10^{-12} am $^{-2}$ and maximum values as high as 10^{-11} am $^{-2}$ in middle latitudes (Paulikas, et al., 1966; Mozer and Bruston, 1966), 10^{-7} am $^{-2}$ in auroral zones (O'Brien, 1964; Sharp, et al., 1967), and 10^{-12} am $^{-2}$ in polar regions (Reid, 1965). Observations of the polar electrojet magnetic effects indicate high-latitude ionospheric currents in the 100 km altitude region during disturbed periods of the order of 10^5 amperes which are thus of the same order as the basic dynamic currents. This "ring current", mentioned above, which is indicated by global magnetic field variations under disturbed conditions, is estimated to be of the order of 10^6 amperes if it is located in the L5 regions. Assuming that these currents are segments of the same current system (i.e., the ring current and the auroral electrojet are not completely closed at their respective levels), vertical currents into and out of the ionosphere are inferred. Maximum values of cross-sectional areas of the two available vertical current paths in each hemisphere are of the order of 10^{13} m 2 which then infers magnetic-field-oriented vertical currents greater than 10^{-8} amperes m $^{-2}$.

Preliminary inspection of the geometry of this situation indicates that optimum conditions for flow of high-latitude exospheric currents will occur at equinox time (Webb, 1968b). This results from the enhanced polar conductivity of the ionosphere which is denied one or the other polar region at solstice time. That is, the circuit of I_2 is characterized by increased path resistance at solstice time.

6. Conclusions

The considerations presented above provide a coherent global system of electrical currents in the earth's environment. The principal driving force is indicated to be vertical transport of positive ions in the lower ionospheric region. Through the Hall effect, the dynamo currents are powered, and tropospheric and exospheric currents simply represent leakage paths for the basic dynamo currents.

The model of earth electrification presented here is at strong variance with previous concepts of electrical phenomena in the earth's vicinity. In particular, introduction of neutral-electrical interaction as the basic motivating force of the general electrical structure represents a distinct new line of reasoning. Long-held views of thunderstorm processes as the basic energy source for the lower atmosphere and more recent models of magnetospheric processes as the basic energy source of the upper atmosphere lose some of their flavor in light of these new considerations. The idea of an equipotential ionosphere appears at this time to be clearly in error.

The simplest physical considerations would indicate that a unified global electrical structure would be the most likely case. Maintenance of isolated independent electrical systems in various parts of the atmosphere would appear to be a very difficult situation to achieve. Failure of the various segregated models to effect adequate explanations for the observed local electrical structure and particularly for the interface structure which must exist has provided some indication of their inadequacy. Experimental difficulties have in many cases precluded confirmation of postulated structure and today remain the most difficult obstacle to further progress.

REFERENCES

- Akasofu, S. I., and S. Chapman, 1964. "On the Asymmetric Development of Magnetic Storm Fields in Low and Middle Latitudes." Planet. Space Sci., 12, 601-626.
- Blamont, J. E., and C. de Jager, 1961. "Upper Atmosphere Turbulence Determined by Means of Rockets." Ann. Geophys., 17, 134-144.
- Booker, H. G., 1956. "Turbulence in the Ionosphere with Applications to Meteor Trails, Radio Star Scintillations, Auroral Radar Echoes, and Other Phenomena." J. Geophys. Res., 61, 673-692.
- Buneman, O., 1959. "Dissipation of Currents in Ionized Media." Phys. Rev., 115, 503.
- Chalmers, J. A., 1967. Atmospheric Electricity. Pergamon Press, New York, 515.
- Chamberlain, J. W., 1961. Physics of Aurora and Airglow. Academic Press, New York, 441.
- Chapman, S., and J. Bartels, 1962. Geomagnetism. Clarendon Press, Oxford, Vol. 1, 542.
- Cole, R. K., and E. T. Pierce, 1965. "Electrification in the Earth's Atmosphere for Altitudes Between 0 and 100 Kilometers." J. Geophys. Res., 70, 12, 2735-2749.
- Fejer, J. A., 1965. "Motions of Ionization." Physics of the Earth's Upper Atmosphere, edited by C. O. Hines, I. Paghis, T. R. Harty, and J. A. Fejer, Prentice-Hall, New Jersey, 157-175.
- Goldman, J. L., 1968. "The High Speed Updraft - The Key to the Severe Thunderstorm." J. Atmos. Sci., 25, 2, 222-248.
- Grenet, G., 1947. "Essai d'Explication de la Charge Electrique des Nuages d'Orages." Ann. Geophys., 3, 306-307.
- Grenet, G., 1959. "Le Nuage d'Orage: Machine Electrostatique." Meteorologie, 1-53, 45-47.
- Hines, C. O., I. Paghis, T. R. Harty, and J. A. Fejer, 1965. Physics of the Earth's Upper Atmosphere, Prentice-Hall, New Jersey, 434.
- Johnson, F. S., and E. M. Wilkins, 1965. "Thermal Upper Limit on Eddy Diffusion in the Mesosphere and Lower Thermosphere." J. Geophys. Res., 70, 6, 1281-1284.

- Kellog, W. W., 1964. "Pollution of the Upper Atmosphere by Rockets." Space Sci. Rev., 3, 275-316.
- Lettau, Heinz, 1951. "Diffusion in the Upper Atmosphere." Compendium of Meteorology, American Meteorological Society, Boston, 320-333.
- Matsushita, S., 1965. "Global Presentation of the External S_8 and L Current Systems." J. Geophys. Res., 70, 17, 4395-4398.
- Matsushita, S., and H. Maeda, 1965. "On the Geomagnetic Solar Quiet Daily Variation Field During the IGY." J. Geophys. Res., 70, 11, 2535-2558.
- Moore, C. B., B. Vonnegut, and A. T. Botka, 1958. "Results of an Experiment to Determine Initial Precedence of Organized Electrification and Precipitation in Thunderstorms." Recent Advances in Atmospheric Electricity, Pergamon Press, ed. L. G. Smith, 531.
- Moore, C. B., B. Vonnegut, B. A. Stein, and H. J. Survilar, 1960. "Observations of Electrification and Lightning in Warm Clouds." J. Geophys. Res., 65, 7, 1907-1910.
- Moore, C. B., B. Vonnegut, J. A. Machado, and H. J. Survilas, 1962. "Radar Observations of Rain Gushes Following Overhead Lightning Strokes." J. Geophys. Res., 67, 1, 207-220.
- Mozer, F. S., and P. Bruston, 1966. "Observation of the Low-Altitude Acceleration of Auroral Protons." J. Geophys. Res., 71, 9, 2201-2206.
- O'Brien, B. J., 1964. "High-Latitude Geophysical Studies with Satellite Injun 3. Part 3. Precipitation of Electrons into the Atmosphere." J. Geophys. Res., 69, 13.
- Paulikas, G. A., J. B. Blake, and S. C. Freden, 1966. "Precipitation of Energetic Electrons at Middle Latitudes." J. Geophys. Res., 71, 13, 3165-3172.
- Redding, J. L., 1967. "Diurnal Variation of Telluric Currents near the Magnetic Equator." J. Atmos. Terr. Phys., 29, 297-305.
- Reid, G. C., 1965. "Solar Cosmic Rays and the Ionosphere." Physics of the Earth's Upper Atmosphere, edited by C. O. Hines, I. Paghis, T. R. Harty, and J. A. Fejer, Prentice-Hall, New Jersey, 245-270.
- Sharp, R. D., R. G. Johnson, M. F. Shea, and G. B. Shook, 1967. "Satellite Measurements of Precipitating Protons in the Auroral Zone." J. Geophys. Res., 72, 1, 227-237.
- Stergis, C. G., G. C. Rein, and T. Kangas, 1957. "Electric Field Measurements above Thunderstorms." J. Atmos. Terr. Phys., 11, 83-90.

- Swift, D. L., 1965. "A Mechanism for Energizing Electrons in the Magnetosphere." J. Geophys. Res., 70, 3061.
- Vestine, E. H., L. Laporte, I. Longe, and W. E. Scott, 1947. The Geomagnetic Field, Its Description and Analysis. Carnegie Institution of Washington, Publication No. 580, Washington, D. C.
- Vonnegut, B., 1955. "Possible Mechanism for the Formation of Thunderstorm Electricity." Proc. Conf. Atmospheric Elec., Portsmouth, N. H., Geophysics Research Paper 42, AFCRC-TR-55-222, 169-181, Air Force Cambridge Research Laboratories, Bedford, Mass.
- Vonnegut, B., Charles B. Moore, and A. T. Botka, 1959. "Preliminary Results of an Experiment to Determine Initial Precedence of Organized Electrification and Precipitation in Thunderstorms." J. Geophys. Res., 64, 3, 347-357.
- Vonnegut, B., and C. B. Moore, 1960. "A Possible Effect of Lightning Discharges on Precipitation Formation Process." American Geophysical Union, Monograph No. 5, Physics of Precipitation, 287-290.
- Vonnegut, B., K. Maynard, W. G. Sykes, and C. B. Moore, 1961. "Technique for Introducing Low-Density Space Charge into the Atmosphere." J. Geophys. Res., 66, 3, 823-830.
- Webb, W. L., 1968a. Atmospheric Diurnal Electrical Structure. Space Research VIII, North-Holland Publishing Company, Amsterdam, 896-906.
- Webb, W. L., 1968b. "Source of Atmospheric Electrification." J. Geophys. Res., 73, 16, 5061-5071.
- Webb, W. L., 1969. "Global Electrical Structure." Planetary Electrodynamics, edited by S. C. Coroniti and J. Hughes, Gordon Breach, London.
- Wilson, C. G., 1958. Electricity and Magnetism. The English Universities Press, Ltd., London, 538.
- Wright, J. W., 1962. Mean Electron Density Variation of the Quiet Ionosphere. Technical Note No. 40-13, National Bureau of Standards, Boulder, Colorado.
- Zimmerman, S. P., and K. S. W. Champion, 1963. "Transport Processes in the Upper Atmosphere." J. Geophys. Res., 68, 10, 3049-3056.

ATMOSPHERIC SCIENCES RESEARCH PAPERS

1. Webb, W.L., "Development of Droplet Size Distributions in the Atmosphere," June 1954.
2. Hansen, F. V., and H. Rachele, "Wind Structure Analysis and Forecasting Methods for Rockets," June 1954.
3. Webb, W. L., "Net Electrification of Water Droplets at the Earth's Surface," *J. Meteorol.*, December 1954.
4. Mitchell, R., "The Determination of Non-Ballistic Projectile Trajectories," March 1955.
5. Webb, W. L., and A. McPike, "Sound Ranging Technique for Determining the Trajectory of Supersonic Missiles," #1, March 1955.
6. Mitchell, R., and W. L. Webb, "Electromagnetic Radiation through the Atmosphere," #1, April 1955.
7. Webb, W. L., A. McPike, and H. Thompson, "Sound Ranging Technique for Determining the Trajectory of Supersonic Missiles," #2, July 1955.
8. Barichivich, A., "Meteorological Effects on the Refractive Index and Curvature of Microwaves in the Atmosphere," August 1955.
9. Webb, W. L., A. McPike and H. Thompson, "Sound Ranging Technique for Determining the Trajectory of Supersonic Missiles," #3, September 1955.
10. Mitchell, R., "Notes on the Theory of Longitudinal Wave Motion in the Atmosphere," February 1956.
11. Webb, W. L., "Particulate Counts in Natural Clouds," *J. Meteorol.*, April 1956.
12. Webb, W. L., "Wind Effect on the Aerobee," #1, May 1956.
13. Rachele, H., and L. Anderson, "Wind Effect on the Aerobee," #2, August 1956.
14. Beyers, N., "Electromagnetic Radiation through the Atmosphere," #2, January 1957.
15. Hansen, F. V., "Wind Effect on the Aerobee," #3, January 1957.
16. Kershner, J., and H. Bear, "Wind Effect on the Aerobee," #4, January 1957.
17. Hoidale, G., "Electromagnetic Radiation through the Atmosphere," #3, February 1957.
18. Querfeld, C. W., "The Index of Refraction of the Atmosphere for 2.2 Micron Radiation," March 1957.
19. White, Lloyd, "Wind Effect on the Aerobee," #5, March 1957.
20. Kershner, J. G., "Development of a Method for Forecasting Component Ballistic Wind," August 1957.
21. Layton, Ivan, "Atmospheric Particle Size Distribution," December 1957.
22. Rachele, Henry and W. H. Hatch, "Wind Effect on the Aerobee," #6, February 1958.
23. Beyers, N. J., "Electromagnetic Radiation through the Atmosphere," #4, March 1958.
24. Prosser, Shirley J., "Electromagnetic Radiation through the Atmosphere," #5, April 1958.
25. Armendariz, M., and P. H. Taft, "Double Theodolite Ballistic Wind Computations," June 1958.
26. Jenkins, K. R. and W. L. Webb, "Rocket Wind Measurements," June 1958.
27. Jenkins, K. R., "Measurement of High Altitude Winds with Loki," July 1958.
28. Hoidale, G., "Electromagnetic Propagation through the Atmosphere," #6, February 1959.
29. McLardie, M., R. Helvey, and L. Traylor, "Low-Level Wind Profile Prediction Techniques," #1, June 1959.
30. Lamberth, Roy, "Gustiness at White Sands Missile Range," #1, May 1959.
31. Beyers, N. J., B. Hinds, and G. Hoidale, "Electromagnetic Propagation through the Atmosphere," #7, June 1959.
32. Beyers, N. J., "Radar Refraction at Low Elevation Angles (U)," Proceedings of the Army Science Conference, June 1959.
33. White, L., O. W. Thiele and P. H. Taft, "Summary of Ballistic and Meteorological Support During IGY Operations at Fort Churchill, Canada," August 1959.
34. Hainline, D. A., "Drag Cord-Aerovane Equation Analysis for Computer Application," August 1959.
35. Hoidale, G. B., "Slope-Valley Wind at WSMR," October 1959.
36. Webb, W. L., and K. R. Jenkins, "High Altitude Wind Measurements," *J. Meteorol.*, 16, 5, October 1959.

37. White, Lloyd, "Wind Effect on the Aerobee," #9, October 1959.
38. Webb, W. L., J. W. Coffman, and G. Q. Clark, "A High Altitude Acoustic Sensing System," December 1959.
39. Webb, W. L., and K. R. Jenkins, "Application of Meteorological Rocket Systems," *J. Geophys. Res.*, 64, 11, November 1959.
40. Duncan, Louis, "Wind Effect on the Aerobee," #10, February 1960.
41. Helvey, R. A., "Low-Level Wind Profile Prediction Techniques," #2, February 1960.
42. Webb, W. L., and K. R. Jenkins, "Rocket Sounding of High-Altitude Parameters," *Proc. GM Rel. Symp.*, Dept. of Defense, February 1960.
43. Armendariz, M., and H. H. Monahan, "A Comparison Between the Double Theodolite and Single-Theodolite Wind Measuring Systems," April 1960.
44. Jenkins, K. R., and P. H. Taft, "Weather Elements in the Tularosa Basin," July 1960.
45. Beyers, N. J., "Preliminary Radar Performance Data on Passive Rocket-Borne Wind Sensors," *IRE TRANS, MIL ELECT, MIL-4*, 2-3, April-July 1960.
46. Webb, W. L., and K. R. Jenkins, "Speed of Sound in the Stratosphere," June 1960.
47. Webb, W. L., K. R. Jenkins, and G. Q. Clark, "Rocket Sounding of High Atmosphere Meteorological Parameters," *IRE Trans. Mil. Elect.*, MIL-4, 2-3, April-July 1960.
48. Helvey, R. A., "Low-Level Wind Profile Prediction Techniques," #3, September 1960.
49. Beyers, N. J., and O. W. Thiele, "Meteorological Wind Sensors," August 1960.
50. Armijo, Larry, "Determination of Trajectories Using Range Data from Three Non-colinear Radar Stations," September 1960.
51. Carnes, Patsy Sue, "Temperature Variations in the First 200 Feet of the Atmosphere in an Arid Region," July 1961.
52. Springer, H. S., and R. O. Olsen, "Launch Noise Distribution of Nike-Zeus Missiles," July 1961.
53. Thiele, O. W., "Density and Pressure Profiles Derived from Meteorological Rocket Measurements," September 1961.
54. Diamond, M. and A. B. Gray, "Accuracy of Missile Sound Ranging," November 1961.
55. Lamberth, R. L. and D. R. Veith, "Variability of Surface Wind in Short Distances," #1, October 1961.
56. Swanson, R. N., "Low-Level Wind Measurements for Ballistic Missile Application," January 1962.
57. Lamberth, R. L. and J. H. Grace, "Gustiness at White Sands Missile Range," #2, January 1962.
58. Swanson, R. N. and M. M. Hoidale, "Low-Level Wind Profile Prediction Techniques," #4, January 1962.
59. Rachele, Henry, "Surface Wind Model for Unguided Rockets Using Spectrum and Cross Spectrum Techniques," January 1962.
60. Rachele, Henry, "Sound Propagation through a Windy Atmosphere," #2, February 1962.
61. Webb, W. L., and K. R. Jenkins, "Sonic Structure of the Mesosphere," *J. Acous. Soc. Amer.*, 34, 2, February 1962.
62. Tourin, M. H. and M. M. Hoidale, "Low-Level Turbulence Characteristics at White Sands Missile Range," April 1962.
63. Miers, Bruce T., "Mesospheric Wind Reversal over White Sands Missile Range," March 1962.
64. Fisher, E., R. Lee and H. Rachele, "Meteorological Effects on an Acoustic Wave within a Sound Ranging Array," May 1962.
65. Walter, E. L., "Six Variable Ballistic Model for a Rocket," June 1962.
66. Webb, W. L., "Detailed Acoustic Structure Above the Tropopause," *J. Applied Meteorol.*, 1, 2, June 1962.
67. Jenkins, K. R., "Empirical Comparisons of Meteorological Rocket Wind Sensors," *J. Appl. Meteor.*, June 1962.
68. Lamberth, Roy, "Wind Variability Estimates as a Function of Sampling Interval," July 1962.
69. Rachele, Henry, "Surface Wind Sampling Periods for Unguided Rocket Impact Prediction," July 1962.
70. Traylor, Larry, "Coriolis Effects on the Aerobee-Hi Sounding Rocket," August 1962.
71. McCoy, J., and G. Q. Clark, "Meteorological Rocket Thermometry," August 1962.
72. Rachele, Henry, "Real-Time Prelaunch Impact Prediction System," August 1962.

73. Beyers, N. J., O. W. Thiele, and N. K. Wagner, "Performance Characteristics of Meteorological Rocket Wind and Temperature Sensors," October 1962.
74. Coffman, J., and R. Price, "Some Errors Associated with Acoustical Wind Measurements through a Layer," October 1962.
75. Armendariz, M., E. Fisher, and J. Serna, "Wind Shear in the Jet Stream at WS-MR," November 1962.
76. Armendariz, M., F. Hansen, and S. Carnes, "Wind Variability and its Effect on Rocket Impact Prediction," January 1963.
77. Querfeld, C., and Wayne Yunker, "Pure Rotational Spectrum of Water Vapor, I: Table of Line Parameters," February 1963.
78. Webb, W. L., "Acoustic Component of Turbulence," *J. Applied Meteorol.*, 2, 2, April 1963.
79. Beyers, N. and L. Engberg, "Seasonal Variability in the Upper Atmosphere," May 1963.
80. Williamson, L. E., "Atmospheric Acoustic Structure of the Sub-polar Fall," May 1963.
81. Lamberth, Roy and D. Veith, "Upper Wind Correlations in Southwestern United States," June 1963.
82. Sandlin, E., "An analysis of Wind Shear Differences as Measured by AN/FPS-16 Radar and AN/GMD-1B Rawinsonde," August 1963.
83. Diamond, M. and R. P. Lee, "Statistical Data on Atmospheric Design Properties Above 30 km," August 1963.
84. Thiele, O. W., "Mesospheric Density Variability Based on Recent Meteorological Rocket Measurements," *J. Applied Meteorol.*, 2, 5, October 1963.
85. Diamond, M., and O. Essenwanger, "Statistical Data on Atmospheric Design Properties to 30 km," *Astro. Aero. Engr.*, December 1963.
86. Hansen, F. V., "Turbulence Characteristics of the First 62 Meters of the Atmosphere," December 1963.
87. Morris, J. E., and B. T. Miers, "Circulation Disturbances Between 25 and 70 kilometers Associated with the Sudden Warming of 1963," *J. of Geophys. Res.*, January 1964.
88. Thiele, O. W., "Some Observed Short Term and Diurnal Variations of Stratospheric Density Above 30 km," January 1964.
89. Sandlin, R. E., Jr. and E. Armijo, "An Analysis of AN/FPS-16 Radar and AN/GMD-1B Rawinsonde Data Differences," January 1964.
90. Miers, B. T., and N. J. Beyers, "Rocketsonde Wind and Temperature Measurements Between 30 and 70 km for Selected Stations," *J. Applied Meteorol.*, February 1964.
91. Webb, W. L., "The Dynamic Stratosphere," *Astronautics and Aerospace Engineering*, March 1964.
92. Low, R. D. H., "Acoustic Measurements of Wind through a Layer," March 1964.
93. Diamond, M., "Cross Wind Effect on Sound Propagation," *J. Applied Meteorol.*, April 1964.
94. Lee, R. P., "Acoustic Ray Tracing," April 1964.
95. Reynolds, R. D., "Investigation of the Effect of Lapse Rate on Balloon Ascent Rate," May 1964.
96. Webb, W. L., "Scale of Stratospheric Detail Structure," *Space Research V*, May 1964.
97. Barber, T. L., "Proposed X-Ray-Infrared Method for Identification of Atmospheric Mineral Dust," June 1964.
98. Thiele, O. W., "Ballistic Procedures for Unguided Rocket Studies of Nuclear Environments (U)," Proceedings of the Army Science Conference, June 1964.
99. Horn, J. D., and E. J. Trawle, "Orographic Effects on Wind Variability," July 1964.
100. Hoidale, G., C. Querfeld, T. Hall, and R. Mireles, "Spectral Transmissivity of the Earth's Atmosphere in the 250 to 500 Wave Number Interval," #1, September 1964.
101. Duncan, L. D., R. Ensey, and B. Engebos, "Athena Launch Angle Determination," September 1964.
102. Thiele, O. W., "Feasibility Experiment for Measuring Atmospheric Density Through the Altitude Range of 60 to 100 KM Over White Sands Missile Range," October 1964.
103. Duncan, L. D., and R. Ensey, "Six-Degree-of-Freedom Digital Simulation Model for Unguided, Fin-Stabilized Rockets," November 1964.

104. Hoidale, G., C. Querfeld, T. Hall, and R. Mireles, "Spectral Transmissivity of the Earth's Atmosphere in the 250 to 500 Wave Number Interval," #2, November 1964.
105. Webb, W. L., "Stratospheric Solar Response," *J. Atmos. Sci.*, November 1964.
106. McCoy, J. and G. Clark, "Rocketsonde Measurement of Stratospheric Temperature," December 1964.
107. Farone, W. A., "Electromagnetic Scattering from Radially Inhomogeneous Spheres as Applied to the Problem of Clear Atmosphere Radar Echoes," December 1964.
108. Farone, W. A., "The Effect of the Solid Angle of Illumination or Observation on the Color Spectra of 'White Light' Scattered by Cylinders," January 1965.
109. Williamson, L. E., "Seasonal and Regional Characteristics of Acoustic Atmospheres," *J. Geophys. Res.*, January 1965.
110. Armendariz, M., "Ballistic Wind Variability at Green River, Utah," January 1965.
111. Low, R. D. H., "Sound Speed Variability Due to Atmospheric Composition," January 1965.
112. Querfeld, C. W., "Mie Atmospheric Optics," *J. Opt. Soc. Amer.*, January 1965.
113. Coffman, J., "A Measurement of the Effect of Atmospheric Turbulence on the Coherent Properties of a Sound Wave," January 1965.
114. Rachele, H., and D. Veith, "Surface Wind Sampling for Unguided Rocket Impact Prediction," January 1965.
115. Ballard, H., and M. Izquierdo, "Reduction of Microphone Wind Noise by the Generation of a Proper Turbulent Flow," February 1965.
116. Mireles, R., "An Algorithm for Computing Half Widths of Overlapping Lines on Experimental Spectra," February 1965.
117. Richart, H., "Inaccuracies of the Single-Theodolite Wind Measuring System in Ballistic Application," February 1965.
118. D'Arcy, M., "Theoretical and Practical Study of Aerobee-150 Ballistics," March 1965.
119. McCoy, J., "Improved Method for the Reduction of Rocketsonde Temperature Data," March 1965.
120. Mireles, R., "Uniqueness Theorem in Inverse Electromagnetic Cylindrical Scattering," April 1965.
121. Coffman, J., "The Focusing of Sound Propagating Vertically in a Horizontally Stratified Medium," April 1965.
122. Farone, W. A., and C. Querfeld, "Electromagnetic Scattering from an Infinite Circular Cylinder at Oblique Incidence," April 1965.
123. Rachele, H., "Sound Propagation through a Windy Atmosphere," April 1965.
124. Miers, B., "Upper Stratospheric Circulation over Ascension Island," April 1965.
125. Rider, L., and M. Armendariz, "A Comparison of Pibal and Tower Wind Measurements," April 1965.
126. Hoidale, G. B., "Meteorological Conditions Allowing a Rare Observation of 24 Micron Solar Radiation Near Sea Level," *Meteorol. Magazine*, May 1965.
127. Beyers, N. J., and B. T. Miers, "Diurnal Temperature Change in the Atmosphere Between 30 and 60 km over White Sands Missile Range," *J. Atmos. Sci.*, May 1965.
128. Querfeld, C., and W. A. Farone, "Tables of the Mie Forward Lobe," May 1965.
129. Farone, W. A., "Generalization of Rayleigh-Gans Scattering from Radially Inhomogeneous Spheres," *J. Opt. Soc. Amer.*, June 1965.
130. Diamond, M., "Note on Mesospheric Winds Above White Sands Missile Range," *J. Applied Meteorol.*, June 1965.
131. Clark, G. Q., and J. G. McCoy, "Measurement of Stratospheric Temperature," *J. Applied Meteorol.*, June 1965.
132. Hall, T., G. Hoidale, R. Mireles, and C. Querfeld, "Spectral Transmissivity of the Earth's Atmosphere in the 250 to 500 Wave Number Interval," #3, July 1965.
133. McCoy, J., and C. Tate, "The Delta-T Meteorological Rocket Payload," June 1964.
134. Horn, J. D., "Obstacle Influence in a Wind Tunnel," July 1965.
135. McCoy, J., "An AC Probe for the Measurement of Electron Density and Collision Frequency in the Lower Ionosphere," July 1965.
136. Miers, B. T., M. D. Kays, O. W. Thiele and E. M. Newby, "Investigation of Short Term Variations of Several Atmospheric Parameters Above 30 KM," July 1965.

137. Serna, J., "An Acoustic Ray Tracing Method for Digital Computation," September 1965.
138. Webb, W. L., "Morphology of Noctilucent Clouds," *J. Geophys. Res.*, 70, 18, 4463-4475, September 1965.
139. Kays, M., and R. A. Craig, "On the Order of Magnitude of Large-Scale Vertical Motions in the Upper Stratosphere," *J. Geophys. Res.*, 70, 18, 4455-4462, September 1965.
140. Rider, L., "Low-Level Jet at White Sands Missile Range," September 1965.
141. Lamberth, R. L., R. Reynolds, and Morton Wurtele, "The Mountain Lee Wave at White Sands Missile Range," *Bull. Amer. Meteorol. Soc.*, 46, 10, October 1965.
142. Reynolds, R. and R. L. Lamberth, "Ambient Temperature Measurements from Radiosondes Flown on Constant-Level Balloons," October 1965.
143. McCluney, E., "Theoretical Trajectory Performance of the Five-Inch Gun Probe System," October 1965.
144. Pena, R. and M. Diamond, "Atmospheric Sound Propagation near the Earth's Surface," October 1965.
145. Mason, J. B., "A Study of the Feasibility of Using Radar Chaff For Stratospheric Temperature Measurements," November 1965.
146. Diamond, M., and R. P. Lee, "Long-Range Atmospheric Sound Propagation," *J. Geophys. Res.*, 70, 22, November 1965.
147. Lamberth, R. L., "On the Measurement of Dust Devil Parameters," November 1965.
148. Hansen, F. V., and P. S. Hansen, "Formation of an Internal Boundary over Heterogeneous Terrain," November 1965.
149. Webb, W. L., "Mechanics of Stratospheric Seasonal Reversals," November 1965.
150. U. S. Army Electronics R & D Activity, "U. S. Army Participation in the Meteorological Rocket Network," January 1966.
151. Rider, L. J., and M. Armendariz, "Low-Level Jet Winds at Green River, Utah," February 1966.
152. Webb, W. L., "Diurnal Variations in the Stratospheric Circulation," February 1966.
153. Beyers, N. J., B. T. Miers, and R. J. Reed, "Diurnal Tidal Motions near the Stratosopause During 48 Hours at WSMR," February 1966.
154. Webb, W. L., "The Stratospheric Tidal Jet," February 1966.
155. Hall, J. T., "Focal Properties of a Plane Grating in a Convergent Beam," February 1966.
156. Duncan, L. D., and Henry Rachele, "Real-Time Meteorological System for Firing of Unguided Rockets," February 1966.
157. Kays, M. D., "A Note on the Comparison of Rocket and Estimated Geostrophic Winds at the 10-mb Level," *J. Appl. Meteor.*, February 1966.
158. Rider, L., and M. Armendariz, "A Comparison of Pibal and Tower Wind Measurements," *J. Appl. Meteor.*, 5, February 1966.
159. Duncan, L. D., "Coordinate Transformations in Trajectory Simulations," February 1966.
160. Williamson, L. E., "Gun-Launched Vertical Probes at White Sands Missile Range," February 1966.
161. Randhawa, J. S., "Ozone Measurements with Rocket-Borne Ozonesondes," March 1966.
162. Armendariz, Manuel, and Laurence J. Rider, "Wind Shear for Small Thickness Layers," March 1966.
163. Low, R. D. H., "Continuous Determination of the Average Sound Velocity over an Arbitrary Path," March 1966.
164. Hansen, Frank V., "Richardson Number Tables for the Surface Boundary Layer," March 1966.
165. Cochran, V. C., E. M. D'Arcy, and Florencio Ramirez, "Digital Computer Program for Five-Degree-of-Freedom Trajectory," March 1966.
166. Thiele, O. W., and N. J. Beyers, "Comparison of Rocketsonde and Radiosonde Temperatures and a Verification of Computed Rocketsonde Pressure and Density," April 1966.
167. Thiele, O. W., "Observed Diurnal Oscillations of Pressure and Density in the Upper Stratosphere and Lower Mesosphere," April 1966.
168. Kays, M. D., and R. A. Craig, "On the Order of Magnitude of Large-Scale Vertical Motions in the Upper Stratosphere," *J. Geophys. Res.*, April 1966.
169. Hansen, F. V., "The Richardson Number in the Planetary Boundary Layer," May 1966.

170. Ballard, H. N., "The Measurement of Temperature in the Stratosphere and Mesosphere," June 1966.
171. Hansen, Frank V., "The Ratio of the Exchange Coefficients for Heat and Momentum in a Homogeneous, Thermally Stratified Atmosphere," June 1966.
172. Hansen, Frank V., "Comparison of Nine Profile Models for the Diabatic Boundary Layer," June 1966.
173. Rachele, Henry, "A Sound-Ranging Technique for Locating Supersonic Missiles," May 1966.
174. Farone, W. A., and C. W. Querfeld, "Electromagnetic Scattering from Inhomogeneous Infinite Cylinders at Oblique Incidence," *J. Opt. Soc. Amer.* 56, 4, 476-480, April 1966.
175. Mireles, Ramon, "Determination of Parameters in Absorption Spectra by Numerical Minimization Techniques," *J. Opt. Soc. Amer.* 56, 5, 644-647, May 1966.
176. Reynolds, R., and R. L. Lamberth, "Ambient Temperature Measurements from Radiosondes Flown on Constant-Level Balloons," *J. Appl. Meteorol.*, 5, 3, 304-307, June 1966.
177. Hall, James T., "Focal Properties of a Plane Grating in a Convergent Beam," *Appl. Opt.*, 5, 1051, June 1966.
178. Rider, Laurence J., "Low-Level Jet at White Sands Missile Range," *J. Appl. Meteorol.*, 5, 3, 283-287, June 1966.
179. McCluney, Eugene, "Projectile Dispersion as Caused by Barrel Displacement in the 5-Inch Gun Probe System," July 1966.
180. Armendariz, Manuel, and Laurence J. Rider, "Wind Shear Calculations for Small Shear Layers," June 1966.
181. Lamberth, Roy L., and Manuel Armendariz, "Upper Wind Correlations in the Central Rocky Mountains," June 1966.
182. Hansen, Frank V., and Virgil D. Lang, "The Wind Regime in the First 62 Meters of the Atmosphere," June 1966.
183. Randhawa, Jagir S., "Rocket-Borne Ozonesonde," July 1966.
184. Rachele, Henry, and L. D. Duncan, "The Desirability of Using a Fast Sampling Rate for Computing Wind Velocity from Pilot-Balloon Data," July 1966.
185. Hinds, B. D., and R. G. Pappas, "A Comparison of Three Methods for the Correction of Radar Elevation Angle Refraction Errors," August 1966.
186. Riedmuller, G. F., and T. L. Barber, "A Mineral Transition in Atmospheric Dust Transport," August 1966.
187. Hall, J. T., C. W. Querfeld, and G. B. Hoidale, "Spectral Transmissivity of the Earth's Atmosphere in the 250 to 500 Wave Number Interval," Part IV (Final), July 1966.
188. Duncan, L. D. and B. F. Engebos, "Techniques for Computing Launcher Settings for Unguided Rockets," September 1966.
189. Duncan, L. D., "Basic Considerations in the Development of an Unguided Rocket Trajectory Simulation Model," September 1966.
190. Miller, Walter B., "Consideration of Some Problems in Curve Fitting," September 1966.
191. Cermak, J. E., and J. D. Horn, "The Tower Shadow Effect," August 1966.
192. Webb, W. L., "Stratospheric Circulation Response to a Solar Eclipse," October 1966.
193. Kennedy, Bruce, "Muzzle Velocity Measurement," October 1966.
194. Traylor, Larry E., "A Refinement Technique for Unguided Rocket Drag Coefficients," October 1966.
195. Nusbaum, Henry, "A Reagent for the Simultaneous Microscope Determination of Quartz and Halides," October 1966.
196. Kays, Marvin and R. O. Olsen, "Improved Rocketsonde Parachute-derived Wind Profiles," October 1966.
197. Engebos, Berna F. and Duncan, Louis D., "A Nomogram for Field Determination of Launcher Angles for Unguided Rockets," October 1966.
198. Webb, W. L., "Midlatitude Clouds in the Upper Atmosphere," November 1966.
199. Hansen, Frank V., "The Lateral Intensity of Turbulence as a Function of Stability," November 1966.
200. Rider, L. J. and M. Armendariz, "Differences of Tower and Pibal Wind Profiles," November 1966.
201. Lee, Robert P., "A Comparison of Eight Mathematical Models for Atmospheric Acoustical Ray Tracing," November 1966.
202. Low, R. D. H., et al., "Acoustical and Meteorological Data Record, SOTRAN I and II," November 1966.

203. Hunt, J. A. and J. D. Horn, "Drag Plate Balance," December 1966.
204. Armendariz, M., and H. Rachele, "Determination of a Representative Wind Profile from Balloon Data," December 1966.
205. Hansen, Frank V., "The Aerodynamic Roughness of the Complex Terrain of White Sands Missile Range," January 1967.
206. Morris, James E., "Wind Measurements in the Subpolar Mesopause Region," January 1967.
207. Hall, James T., "Attenuation of Millimeter Wavelength Radiation by Gaseous Water," January 1967.
208. Thiele, O. W., and N. J. Beyers, "Upper Atmosphere Pressure Measurements With Thermal Conductivity Gauges," January 1967.
209. Armendariz, M., and H. Rachele, "Determination of a Representative Wind Profile from Balloon Data," January 1967.
210. Hansen, F. V., "The Aerodynamic Roughness of the Complex Terrain of White Sands Missile Range, New Mexico," January 1967.
211. D'Arcy, Edward M., "Some Applications of Wind to Unguided Rocket Impact Prediction," March 1967.
212. Kennedy, Bruce, "Operation Manual for Stratosphere Temperature Sonde," March 1967.
213. Hoidale, G. B., S. M. Smith, A. J. Blanco, and T. L. Barber, "A Study of Atmospheric Dust," March 1967.
214. Longyear, J. Q., "An Algorithm for Obtaining Solutions to Laplace's Tidal Equations," March 1967.
215. Rider, L. J., "A Comparison of Pibal with Raob and Rawin Wind Measurements," April 1967.
216. Breeland, A. H., and R. S. Bonner, "Results of Tests Involving Hemispherical Wind Screens in the Reduction of Wind Noise," April 1967.
217. Webb, Willis L., and Max C. Bolen, "The D-region Fair-Weather Electric Field," April 1967.
218. Kubinski, Stanley F., "A Comparative Evaluation of the Automatic Tracking Pilot-Balloon Wind Measuring System," April 1967.
219. Miller, Walter B., and Henry Rachele, "On Nonparametric Testing of the Nature of Certain Time Series," April 1967.
220. Hansen, Frank V., "Spatial and Temporal Distribution of the Gradient Richardson Number in the Surface and Planetary Layers," May 1967.
221. Randhawa, Jagir S., "Diurnal Variation of Ozone at High Altitudes," May 1967.
222. Ballard, Harold N., "A Review of Seven Papers Concerning the Measurement of Temperature in the Stratosphere and Mesosphere," May 1967.
223. Williams, Ben H., "Synoptic Analyses of the Upper Stratospheric Circulation During the Late Winter Storm Period of 1966," May 1967.
224. Horn, J. D., and J. A. Hunt, "System Design for the Atmospheric Sciences Office Wind Research Facility," May 1967.
225. Miller, Walter B., and Henry Rachele, "Dynamic Evaluation of Radar and Photo Tracking Systems," May 1967.
226. Bonner, Robert S., and Ralph H. Rohwer, "Acoustical and Meteorological Data Report - SOTRAN III and IV," May 1967.
227. Rider, L. J., "On Time Variability of Wind at White Sands Missile Range, New Mexico," June 1967.
228. Randhawa, Jagir S., "Mesospheric Ozone Measurements During a Solar Eclipse," June 1967.
229. Beyers, N. J., and B. T. Miers, "A Tidal Experiment in the Equatorial Stratosphere over Ascension Island (8S)," June 1967.
230. Miller, W. B., and H. Rachele, "On the Behavior of Derivative Processes," June 1967.
231. Walters, Randall K., "Numerical Integration Methods for Ballistic Rocket Trajectory Simulation Programs," June 1967.
232. Hansen, Frank V., "A Diabatic Surface Boundary Layer Model," July 1967.
233. Butler, Ralph L., and James K. Hall, "Comparison of Two Wind Measuring Systems with the Contraves Photo-Theodolite," July 1967.
234. Webb, Willis L., "The Source of Atmospheric Electrification," June 1967.

235. Harris, B. D., "Radar Tracking Anomalies over an Arid Interior Basin," August 1967.
236. Christian, Larry O., "Radar Cross Sections for Totally Reflecting Spheres," August 1967.
237. D'Arcy, Edward M., "Theoretical Dispersion Analysis of the Aerobee 350," August 1967.
238. Anon., "Technical Data Package for Rocket-Borne Temperature Sensor," August 1967.
239. Glass, Roy L., Roy L. Lamberth, and Ralph D. Reynolds, "A High Resolution Continuous Pressure Sensor Modification for Radiosondes," August 1967.
240. Low, Richard D. H., "Acoustic Measurement of Supersaturation in a Warm Cloud," August 1967.
241. Rubio, Roberto, and Harold N. Ballard, "Time Response and Aerodynamic Heating of Atmospheric Temperature Sensing Elements," August 1967.
242. Seagraves, Mary Ann B., "Theoretical Performance Characteristics and Wind Effects for the Aerobee 150," August 1967.
243. Duncan, Louis Dean, "Channel Capacity and Coding," August 1967.
244. Dunaway, G. L., and Mary Ann B. Seagraves, "Launcher Settings Versus Jack Settings for Aerobee 150 Launchers - Launch Complex 35, White Sands Missile Range, New Mexico," August 1967.
245. Duncan, Louis D., and Bernard F. Engebos, "A Six-Degree-of-Freedom Digital Computer Program for Trajectory Simulation," October 1967.
246. Rider, Laurence J., and Manuel Armandariz, "A Comparison of Simultaneous Wind Profiles Derived from Smooth and Roughened Spheres," September 1967.
247. Reynolds, Ralph D., Roy L. Lamberth, and Morton G. Wurtele, "Mountain Wave Theory vs Field Test Measurements," September 1967.
248. Lee, Robert P., "Probabilistic Model for Acoustic Sound Ranging," October 1967.
249. Williamson, L. Edwin, and Bruce Kennedy, "Meteorological Shell for Standard Artillery Pieces - A Feasibility Study," October 1967.
250. Rohwer, Ralph H., "Acoustical, Meteorological and Seismic Data Report - SOTRAN V and VI," October 1967.
251. Nordquist, Walter S., Jr., "A Study in Acoustic Direction Finding," November 1967.
252. Nordquist, Walter S., Jr., "A Study of Acoustic Monitoring of the Gun Probe System," November 1967.
253. Avara, E. P., and B. T. Miers, "A Data Reduction Technique for Meteorological Wind Data above 30 Kilometers," December 1967.
254. Hansen, Frank V., "Predicting Diffusion of Atmospheric Contaminants by Consideration of Turbulent Characteristics of WSMR," January 1968.
255. Randhawa, Jagat S., "Rocket Measurements of Atmospheric Ozone," January 1968.
256. D'Arcy, Edward M., "Meteorological Requirements for the Aerobee-350," January 1968.
257. D'Arcy, Edward M., "A Computer Study of the Wind Frequency Response of Unguided Rockets," February 1968.
258. Williamson, L. Edwin, "Gun Launched Probes - Parachute Expulsion Tests Under Simulated Environment," February 1968.
259. Beyers, Norman J., Bruce T. Miers, and Elton P. Avara, "The Diurnal Tide Near the Stratopause over White Sands Missile Range, New Mexico," February 1968.
260. Traylor, Larry E., "Preliminary Study of the Wind Frequency Response of the Honest John M59 Tactical Rocket," March 1968.
261. Engebos, B. F., and L. D. Duncan, "Real-Time Computations of Pilot Balloon Winds," March 1968.
262. Better, Ralph and L. D. Duncan, "Empirical Estimates of Errors in Double-Theodolite Wind Measurements," February 1968.
263. Kennedy, Bruce, et al., "Thin Film Temperature Sensor," March 1968.
264. Bruce, Dr. Rufus, James Mason, Dr. Kenneth White and Richard B. Gomez, "An Estimate of the Atmospheric Propagation Characteristics of 1.54 Micron Laser Energy," March 1968.

265. Ballard, Harold N., Jagir S. Randhawa, and Willis L. Webb, "Stratospheric Circulation Response to a Solar Eclipse," March 1968.
266. Johnson, James L., and Orville C. Kuberski, "Timing Controlled Pulse Generator," April 1968.
267. Blanco, Abel J., and Glenn B. Hoidale, "Infrared Absorption Spectra of Atmospheric Dust," May 1968.
268. Jacobs, Willie N., "Automatic Pibal Tracking System," May 1968.
269. Morris, James E., and Marvin D. Kays, "Circulation in the Arctic Mesosphere in Summer," June 1968.
270. Mason, James B., "Detection of Atmospheric Oxygen Using a Tuned Ruby Laser," June 1968.
271. Armendariz, Manuel, and Virgil D. Lang, "Wind Correlation and Variability in Time and Space," July 1968.
272. Webb, Willis L., "Tropospheric Electrical Structure," July 1968.
273. Miers, Bruce T., and Elton P. Avara, "Analysis of High-Frequency Components of AN FPS-16 Radar Data," August 1968.
274. Dunaway, Gordon L., "A Practical Field Wind Compensation Technique for Unguided Rockets," August 1968.
275. Seagraves, Mary Ann B., and Barry Butler, "Performance Characteristics and Wind Effects for the Aerobee 150 with VAM Booster," September 1968.
276. Low, Richard D. H., "A Generalized Equation for Droplet Growth Due to the Solution Effect," September 1968.
277. Jenkins, Kenneth R., "Meteorological Research, Development, Test, and Evaluation Rocket," September 1968.
278. Williams, Ben H., and Bruce T. Miers, "The Synoptic Events of the Stratospheric Warming of December 1967 - January 1968," September 1968.
279. Tate, C. L., and Bruce W. Kennedy, "Technical Data Package for Atmospheric Temperature Sensor Mini-Loki," September 1968.
280. Rider, Laurence J., Manuel Armendariz, and Frank V. Hansen, "A Study of Wind and Temperature Variability at White Sands Missile Range, New Mexico," September 1968.
281. Duncan, Louis D., and Walter B. Miller, "The Hull of a Channel," September 1968.
282. Hansen, Frank V., and Gary A. Ethridge, "Diffusion Nomograms and Tables for Rocket Propellants and Combustion By-Products," January 1968.
283. Walters, Randall K., and Bernard F. Engebos, "An Improved Method of Error Control for Runge-Kutta Numerical Integration," October 1968.
284. Miller, Walter B., "A Non-Entropy Approach to Some Topics in Channel Theory," November 1968.
285. Armendariz, Manuel, Laurence J. Rider, and Frank V. Hansen, "Turbulent Characteristics in the Surface Boundary Layer," November 1968.
286. Randhawa, Jagir S., "Rocket Measurements of the Diurnal Variation of Atmospheric Ozone," December 1968.
287. Randhawa, Jagir S., "A Guide to Rocketsonde Measurements of Atmospheric Ozone," January 1969.
288. Webb, Willis L., "Solar Control of the Stratospheric Circulation," February 1969.
289. Lee, Robert P., "A Dimensional Analysis of the Errors of Atmospheric Sound Ranging," March 1969.
290. Barber, T. L., "Degradation of Laser Optical Surfaces," March 1969.
291. D'Arcy, E. M., "Diffusion of Resonance Excitation Through a One-Dimensional Gas," March 1969.
292. Randhawa, J. S., "Ozone Measurements from a Stable Platform near the Stratosphere Level," March 1969.
293. Rubio, Roberto, "Faraday Rotation System for Measuring Electron Densities," March 1969.
294. Olsen, Robert, "A Design Plan for Investigating the Atmospheric Environment Associated with High Altitude Nuclear Testing," March 1969.
295. Monahan, H. H., M. Armendariz, and V. D. Lang, "Estimates of Wind Variability Between 100 and 900 Meters," April 1969.
296. Rinehart, G. S., "Fog Drop Size Distributions - Measurement Methods and Evaluation," April 1969.

297. D'Arcy, Edward M., and Henry Rachele, "Proposed Prelaunch Real-Time Impact Prediction System for the Aerobee-350 Rocket," May 1969.
298. Low, Richard D. H., "A Comprehensive Report on Nineteen Condensation Nuclei (Part I - Equilibrium Growth and Physical Properties)," May 1969.
299. Randhawa, J. S., "Vertical Distribution of Ozone in the Winter Subpolar Region," June 1969.
300. Rider, Laurence J., and Manuel Armendariz, "Vertical Wind Component Estimates up to 1.2km Above Ground, July 1969.
301. Duncan, L. D., and Bernard F. Engebos, "A Rapidly Converging Iterative Technique for Computing Wind Compensation Launcher Settings for Unguided Rockets," July 1969.
302. Gomez, R. B. and K. O. White, "Erbium Laser Propagation in Simulated Atmospheres I. Description of Experimental Apparatus and Preliminary Results," July 1969.
303. Hansen, Frank V., and Juana Serna, "A Dimensionless Solution for the Wind and Temperature Profiles in the Surface Boundary Layer," September 1969.
304. Webb, Willis L., "Global Electrical Currents," October 1969.

DISTRIBUTION LIST

ID#/CYS

DEPARTMENT OF DEFENSE

101/20* Defense Documentation Center
ATTN: DDC-IRS
Cameron Station (Bldg. 5)
Alexandria, Virginia 22314

102/1 Office of Asst Secretary of Defense
(Research and Engineering)
ATTN: Technical Library, RM 3E1065
Washington, D. C. 20301

103/1 Director, Defense Atomic Support
Agency
ATTN: Document Library Branch
Washington, D. C. 20301

107/1 Department of Defense
Defense Intelligence Agency
ATTN: DIAAP-IES
Washington, D. C. 20301

DEPARTMENT OF THE NAVY

200/1 Chief Of Naval Research
ATTN: Code 427
Department of the Navy
Washington, D. C. 20325

201/1 Naval Ships Systems Command
ATTN: Code 20526 (Technical Library)
Main Navy Building, Room 1528
Washington, D. C. 20325

206/2 Director
U. S. Naval Research Laboratory
ATTN: Code 2027
Washington, D. C. 20390

207/1 Commanding Officer and Director
U. S. Navy Electronics Laboratory
ATTN: Library
San Deigo, California 92101

208.1 Commander
U. S. Naval Ordnance Laboratory
ATTN: Technical Library
White Oak, Silver Spring,
Maryland 20910

210/1 Officer of Naval Weather Service
(Code 80)
Washington Navy Yard (Bldg. 200)
Washington, D. C. 20390

211/1 Officer In Charge
U. S. Navy Weather Research Facility
Building R-48, U. S. Naval Air Station
Nortolk, Virginia 23511

212/1 Commandant Marine Corps (Code A04C)
Headquarters, U. S. Marine Corps
Washington, D. C. 20380

213/1 Director
Marine Corps Landing Force Dev Ctr
ATTN: C-E Division
Marine Corps Schools
Quantico, Virginia 22134

214/1 Commandant, Marine Corps
(Code A02F)
Headquarters, U. S. Marine Corps
Washington, D. C. 20380

215/1 Commander
U. S. Naval Weapons Laboratory
ATTN: KXR
Dahlgren, Virginia 22448

216/1 CH, Bureau of Naval Weapons
ATTN: Code FASS
Department of the Navy
Washington, D. C. 20315

217/1 Office of U. S. Naval Weather Service
U. S. Naval Air Station
Washington, D. C. 20390

218/1 Officer in Charge
U. S. Naval Weather Res Fac
U. S. Naval Air Station, Bldg. R-28
Norfolk, Virginia 23511

DEPARMENT OF THE AIR FORCE

304/2 Electronic Systems Div (ESTI)
L. G. Hanscom Field
Bedford, Mass. 01730

305/1 AFCRL (CREW)
L. G. Hanscom Field
Bedford, Mass. 01730

307/1 HQS, Air Weather Service
ATTN: AWVAE/SIPD
Scott Air Force Base, Illinois 62225

308/1 U. S. Air Force Security Service
ATTN: TSG, VICE ATTN: ESD
San Antonio, Texas 78241

309/1 Air Proving Ground Ctr (PGBPS-12)
ATTN: PGAPI
Eglin Air Force Base, Florida 32542

310/1 Headquarters, AFSC
ATTN: SCTSE
Bolling AFB, D. C. 20332

317/1 Commander, Dept of the Air Force
29th Weather Squadron (MAC)
ATTN: 29WSOP (CWO Schissler/727)
Richards-Begzur AFB, Missouri 64030

318/1 Commander
USAF Air Weather Service (MATS)
ATTN: AWSSS/TIPD
Scott AFB, Illinois 62225

320/1 Commander
Air Force Cambridge Res Laboratories
ATTN: CREW
Bedford, Mass. 01730

*Increase to 50 copies if releasable to CFSTI.
See para 5e (4). ECOMR 70-31, for types of re-
ports not to be sent to DDC.

DEPARTMENT OF THE ARMY	
400/2	Chief of Research and Development Department of the Army Washington, D. C. 20315
402/1	Commanding General U. S. Army Materiel Command ATTN: AMCRD-TV Washington, D. C. 20315
405/1	Commanding General U. S. Army Missile Command ATTN: AMSMU-RR, Bldg. 5429 Redstone Arsenal, Alabama 35809
406/3	Redstone Scientific Info Ctr ATTN: Chief, Document Section U. S. Army Missile Command Redstone Arsenal, Alabama 35809
410/2	Commanding Officer Aberdeen Proving Ground ATTN: Technical Library, Bldg. 313 Aberdeen Proving Ground, Maryland 21005
411/2	Headquarters U. S. Continental Army Command ATTN: AMCMA-RM-3 Washington, D. C. 20315
413/1	Commanding General U. S. Army Combat Dev Com ATTN: CDCMR-E Fort Belvoir, Virginia 22060
414/1	Chief of Research and Development ATTN: CRD-M Department of the Army Washington, D. C. 20310
415/1	Commanding Officer U. S. Army Combat Dev Com Communications Electronics Agency Ft. Monmouth, New Jersey 07703
416/1	Commander U. S. Army Research Office (Durham) Box CM-Duke Station Durham, North Carolina 27706
417/1	Commanding Officer U. S. Army Sec Agcy Combat Dev Actv Arlington Hall Station Arlington, Virginia 22212
418/1	U. S. Army Security Agency ATTN: OACofS, Dev Arlington Hall Station Arlington, Virginia 22212
419/1	U. S. Army Security Agency Processing Center ATTN: IAVAPC-R&D Vint Hill Farms Station Warrenton, Virginia 22186
420/1	Technical Support Directorate ATTN: Technical Library Bldg. 3330, Edgewood Arsenal Maryland 21010
421/2	Commanding Officer U. S. Army Nuclear Defense Lab ATTN: Library Edgewood Arsenal, Maryland 21010
422/1	Harry Diamond Laboratories ATTN: Library Connecticut Avenue and Van Ness St. Washington, D. C. 20438
426/1	Commandant U. S. Army Air Defense School ATTN: C&S Dept, MSI, SCI DIV Fort Bliss, Texas 79916
427/1	Commanding General U. S. Army Electronic Proving Ground ATTN: Technical Info Ctr Fort Huachuca, Arizona 85613
428/1	Commanding General U. S. Army Munitions Command ATTN: AMSMU-RE-R Dover, New Jersey 07801
429/3	Commanding General U. S. Army Test & Eval Command ATTN: AMSTE-EL, FA, NBC Aberdeen Proving Ground, MD 21005
430/1	Commanding Officer U. S. Army Cold Regions R&E Lab ATTN: Library Hanover, New Hampshire 03755
431/1	Commanding General U. S. Army Natick Laboratories ATTN: AMXRE-EG Natick, Mass. 01760
432/2	Commanding Officer U. S. Army Ballistic Research Labs ATTN: AMXBR-B & AMXBR-IA Aberdeen Proving Ground, MD 21005
433/2	Director U.S.A. Engr Waterways Exper Station ATTN: Research Center Library Vicksburg, Mississippi 39180
434/1	Director U. S. Army Munitions Command Operations Research Group Edgewood, Arsenal, MD 21010
435/1	Commanding Officer Frankford Arsenal, Bldg. 201-1 ATTN: SMUFA-N3200 Philadelphia, PA. 19137
436/1	Commanding Officer U. S. Army Picatinny Arsenal ATTN: SMUPA-TVI Dover, New Jersey 07801
437/1	Commanding Officer U. S. Army Dugway Proving Grounds ATTN: Meteorology Division Dugway, Utah 84022
438/1	President U. S. Army Artillery Board Fort Sill, Oklahoma 73503
439/1	Commanding Officer U. S. Army Combat Dev Com Artillery Agency Fort Sill, Oklahoma 73504

440/1 Commandant
U.S. Army Artillery & Missile School
ATTN: Target Acquisition Dept.
Fort Sill, Oklahoma 73504

441/1 Commanding Officer
U.S. Army CDC, CBR Agency
ATTN: Mr. N. W. Bush
Fort McClellan, Alabama 36205

442/1 Chief, A.M. & EW Division
ATTN: USALPG-STEEP TD
Fort Huachuca, Arizona 85613

444/1 Commandant
U.S. Army Chemical Center & School
Micrometeorological Section
Fort McClellan, Alabama 36201

445/1 Commandant
U.S. Army Signal School
ATTN: Meteorological Dept.
Fort Monmouth, New Jersey 07703

448/1 Asst Ch of Staff for Force Development
CBR Nuclear Operations Directorate
Department of the Army
Washington, D. C. 20310

451/1 Asst Secretary of the Army (R&D)
Department of the Army
ATTN: Deputy Asst for Army (R&D)
Washington, D. C. 20315

456/1 Commanding Officer
U. S. Army Limited War Laboratory
Aberdeen Proving Ground, MD. 21005

462/1 Chief, Special Techniques Division
Unconventional Warfare Dept.
U. S. Army Special Warfare School
Ft. Bragg, N. Carolina 28307

500/1 Commanding Officer
U. S. Army Biological Labs
ATTN: CB Cloud Research Office
Ft. Detrick, Frederick, MD. 21701

501/1 Commanding Officer
U. S. Army Biological Labs
ATTN: Tech Library SMUFD-12 TL
Ft. Detrick, Frederick, MD. 21701

502/1 Commanding Officer
U. S. Army CBR Oper Research Group
Army Chemical Center, MD. 21401

503/1 Commanding Officer
U. S. Army Chemical R&D Labs
ATTN: Dir. Development Support
Army Chemical Center, MD. 21401

504/1 Commanding General
U.S. Army Materiel Command
ATTN: AMCRD-RS-ES-A
Washington, D. C. 20315

505/1 Commanding General
U.S. Army Materiel Command
ATTN: AMCRD-DE-MI
Washington, D. C. 20315

506/1 Commanding Officer
U. S. Army Transportation Res Cmd
Fort Eustis, Virginia 23604

507/1 President
U. S. Army Arctic Test Board
Ft. Greely, Delta Junction
Alaska 99737

508/1 Headquarters
U. S. Army Supply & Maintenance Cmd
Dover, New Jersey 07801

509/1 Commanding General
U. S. Army CDC
Combined Arms Group
Ft. Leavenworth, Kansas 66027

510/1 Commanding General
U. S. Army Combat Dev Cmd
Combat Support Group
Ft. Belvoir, Virginia 22060

511/1 Commanding General
U. S. Army Munitions Command
ATTN: AMSMU-RE-4
Dover, New Jersey 07801

512/1 Commanding General
U. S. Army Test & Eval Command
ATTN: NBC Directorate
Aberdeen Proving Ground, MD. 21005

513/1 Commanding General
U. S. Army Natick Laboratories
ATTN: Earth Sciences Division
Natick, Mass. 01762

514/1 Commanding General
Deseret Test Center
ATTN: Design & Analysis Div.
Ft. Douglas, Utah 84113

515/1 Commanding Officer
Fort Detrick
ATTN: Environmental Analysis Ofc.
Frederick, Maryland 21701

U. S. ARMY ELECTRONICS COMMAND

551/1 Commanding General
U. S. Army Electronics Command
ATTN: AMSEL-MR
225 South 18th Street
Philadelphia, PA 19103

556/1 Headquarters
U. S. Army Combat Developments Com
ATTN: CDCLN-EL
Fort Belvoir, Virginia 22060

557/1 USAECOM Liaison Officer
MIT, Bldg 26, Rm 131
77 Massachusetts Avenue
Cambridge, Mass. 02139

560/1 USAECOM Liaison Officer
Aeronautical Systems Division
ATTN: ASDL-9
Wright-Patterson AFB, Ohio 45433

561/1 Chief, Atmos Sciences Res Div
ASL, USAECOM, ATTN: AMSEL-BL-
RD
Ft. Huachuca, Arizona 85613

564/1 Chief, Atmos Sciences Office
Atmospheric Sciences Laboratory
U.S. Army Electronics Command
White Sands Missile Range, N.M. 88002

UNCLASSIFIED

Security Classification

DOCUMENT CONTROL DATA - R & D

(Security classification of title, body of abstract and indexing annotation must be entered when the overall report is classified)

1. ORIGINATING ACTIVITY (Corporate author) U. S. Army Electronics Command Fort Monmouth, New Jersey		2a. REPORT SECURITY CLASSIFICATION Unclassified	
		2b. GROUP	
3. REPORT TITLE GLOBAL ELECTRICAL CURRENTS			
4. DESCRIPTIVE NOTES (Type of report and inclusive dates)			
5. AUTHOR(S) (First name, middle initial, last name) Willis L. Webb			
6. REPORT DATE October 1969		7a. TOTAL NO. OF PAGES 23	7b. NO. OF REFS 40
8a. CONTRACT OR GRANT NO.		8b. ORIGINATOR'S REPORT NUMBER(S) ECOM-5271	
a. PROJECT NO.			
c. Task No. 1T061102B53A-18		9b. OTHER REPORT NO(S) (Any other numbers that may be assigned this report)	
d.			
10. DISTRIBUTION STATEMENT Distribution of this report is unlimited.			
11. SUPPLEMENTARY NOTES		12. SPONSORING MILITARY ACTIVITY Atmospheric Sciences Laboratory U. S. Army Electronics Command White Sands Missile Range, New Mexico	
13. ABSTRACT The atmospheric electrical structure of the earth is postulated to be controlled by a motivating force in the lower ionosphere which is produced by interaction between neutral atmosphere tidal circulations and the ionospheric plasma in the presence of the earth's magnetic field. Associated electric fields power the dynamo currents through the Hall effect with a resulting development of a gross electric potential distribution in the lower ionosphere. Asymmetries in these hemispheric potential distributions result in exospheric current flows in low L-shells, and larger differences in potential produced by dynamo return current flows in high magnetic latitudes result in strong currents through high L-shells between auroral zones. Vertical thunderstorm currents with their associated lightning discharges effectively connect the earth to a low potential region of the dynamo circuit and thus supply the earth with an average negative charge which motivates a leakage tropospheric electrical circuit. In addition, the dynamo currents maintain the magnetic polar regions at different potentials with a resulting electrical exchange with the solar wind through the earth's near space. These considerations indicate that observed electrical and variable magnetic phenomena near the earth are all part of a single comprehensive electrical current system.			

DD FORM 1473

REPLACES DD FORM 1473, 1 JAN 64, WHICH IS OBSOLETE FOR ARMY USE.

UNCLASSIFIED

Security Classification